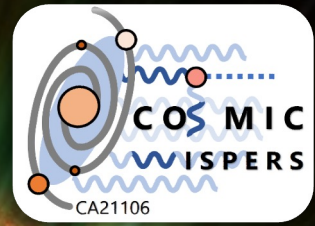




Frascati, 29 July 2025



Core-Collapse Supernovae shining in Axion-like particles

Alessandro Lella

Physics Department of «Aldo Moro» University in Bari
Istituto Nazionale di Fisica Nucleare

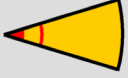


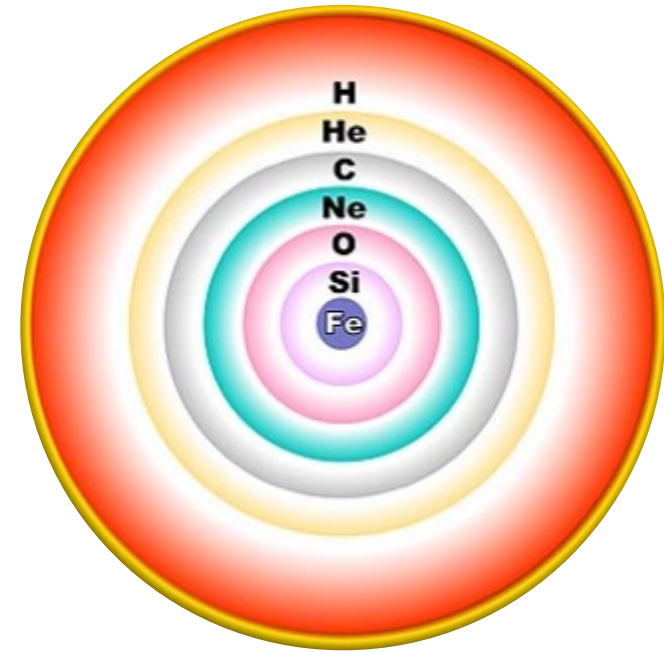
Core-collapse Supernovae

[H.T. Janka & al., Phys.Rept. 442 (2007)]

Massive Stars and Gravitational Collapse

Stars with masses $M \geq 8 M_{\odot}$ can induce heavier elements ignition.

Burning Phase		Dominant Process	T_c [keV]	ρ_c [g/cm ³]	L_{γ} [10 ⁴ L _{sun}]	L_v/L_{γ}	Duration [years]
	Hydrogen	H → He	3	5.9	2.1	–	1.2×10 ⁷
	Helium	He → C, O	14	1.3×10 ³	6.0	1.7×10 ⁻⁵	1.3×10 ⁶
	Carbon	C → Ne, Mg	53	1.7×10 ⁵	8.6	1.0	6.3×10 ³
	Neon	Ne → O, Mg	110	1.6×10 ⁷	9.6	1.8×10 ³	7.0
	Oxygen	O → Si	160	9.7×10 ⁷	9.6	2.1×10 ⁴	1.7
	Silicon	Si → Fe, Ni	270	2.3×10 ⁸	9.6	9.2×10 ⁵	6 days



Heavy elements collected in an “onion” structure with shells of burning elements around a degenerate iron core.

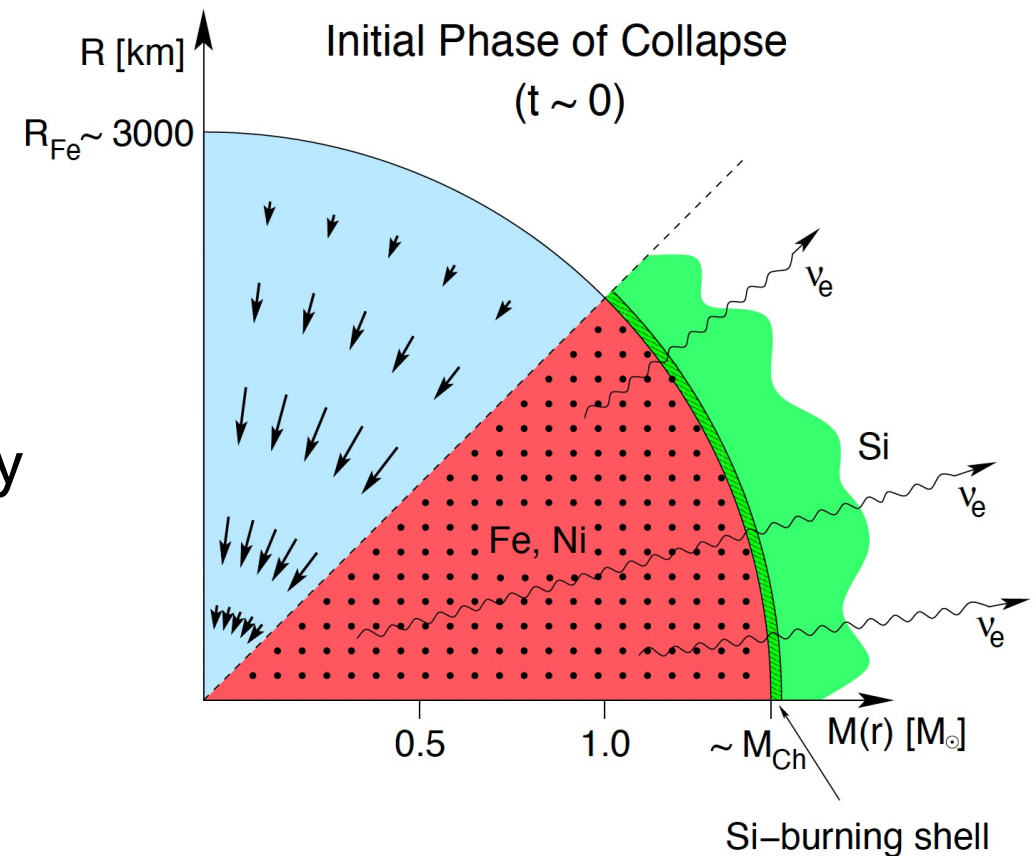
Phases of collapse

Electron degeneracy pressure counter-balances gravity until $M > M_{ch} \sim 5.8 Y_e^2 M_\odot$, ($Y_e \simeq 0.42$).

➤ Instability is mainly due to:

- $e^- + p \rightarrow n + \nu_e$: reduces Y_e and enrich neutron fraction.
- $\gamma + {}^{56}\text{Fe} \rightarrow 13\alpha + 4n$: subtracts energy and reduces degeneracy pressure.

↓
Onset of the Collapse

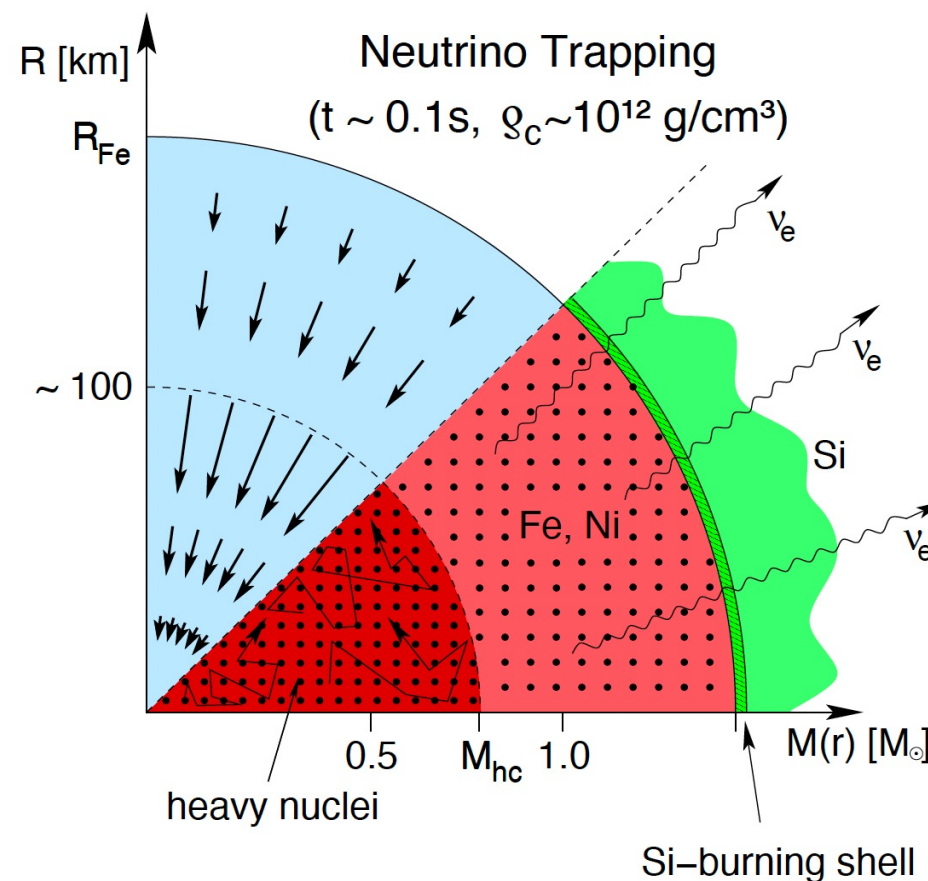


Phases of collapse

β -decays and other processes subtract energy from the core and collapse accelerates.

- Inner (homologous) core collapses at subsonic velocity, while outer layers at supersonic velocity
- When $\rho \sim 10^{12} \text{ g/cm}^{-3}$, ν -diffusion t_ν time is larger than the collapsing time scale t_d

Neutrino Trapping:
Emission from $R_\nu \sim 20 \text{ km}$



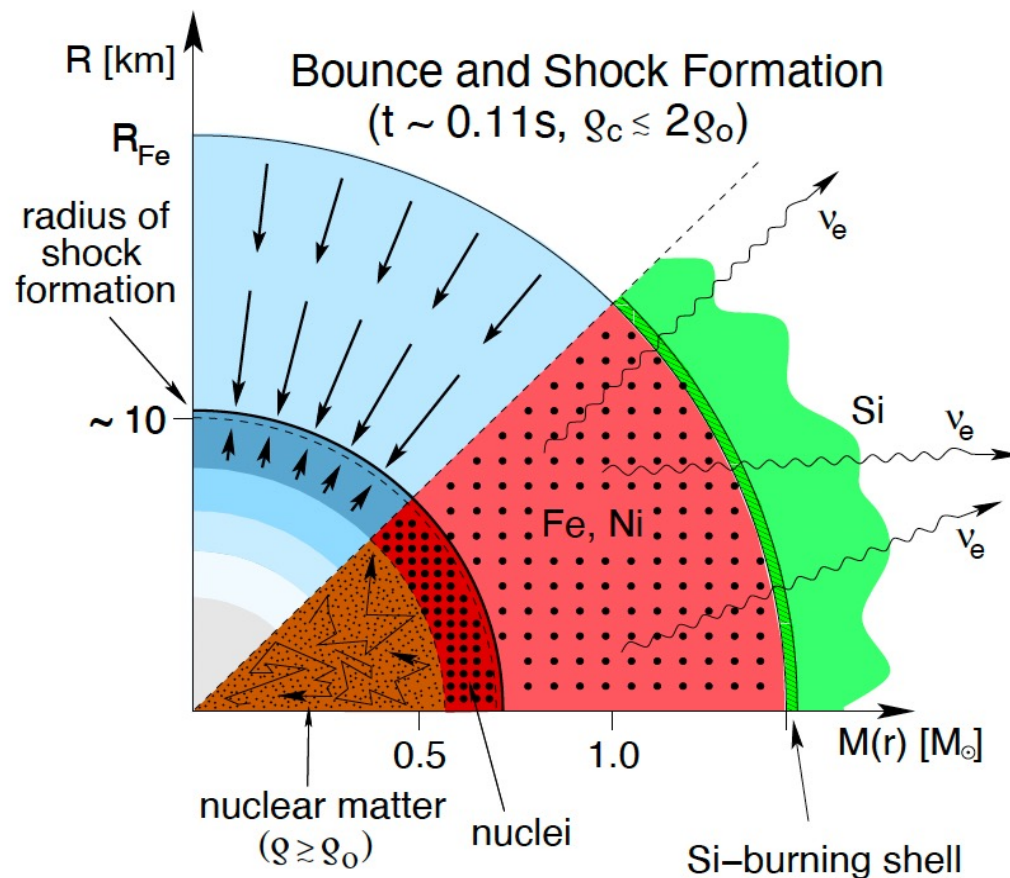
Phases of collapse

Nuclear density in the homologous core increases until $\rho > \rho_c \sim 10^{14} \text{g/cm}^{-3}$.

- Outer layers keep collapsing at supersonic velocity.
- In inner regions nuclear matter becomes incompressible



Formation of a shock-wave



Phases of collapse

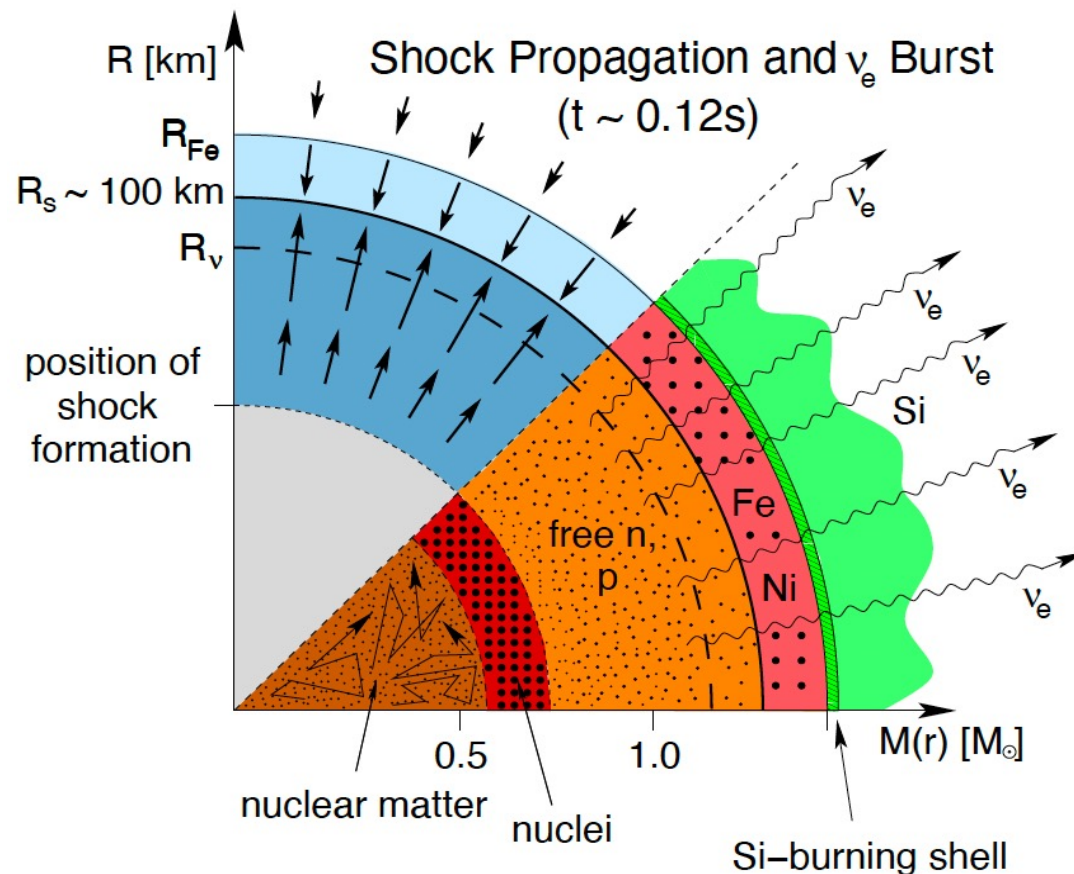
Along its path the shock wave dissociates heavy nuclei in outer layers of the core loosing some of its energy (8.8 MeV per nucleon).

- Reduction of coherent ν -scattering
- Strong enhancement of electron capture on free protons



Prompt ν_e -burst:

Short burst releasing $E \sim 10^{51}$ erg



Phases of collapse

The shock wave loses almost all of its energy and stalls at $R_s \sim 200$ Km

➤ Matter keeps infalling from above



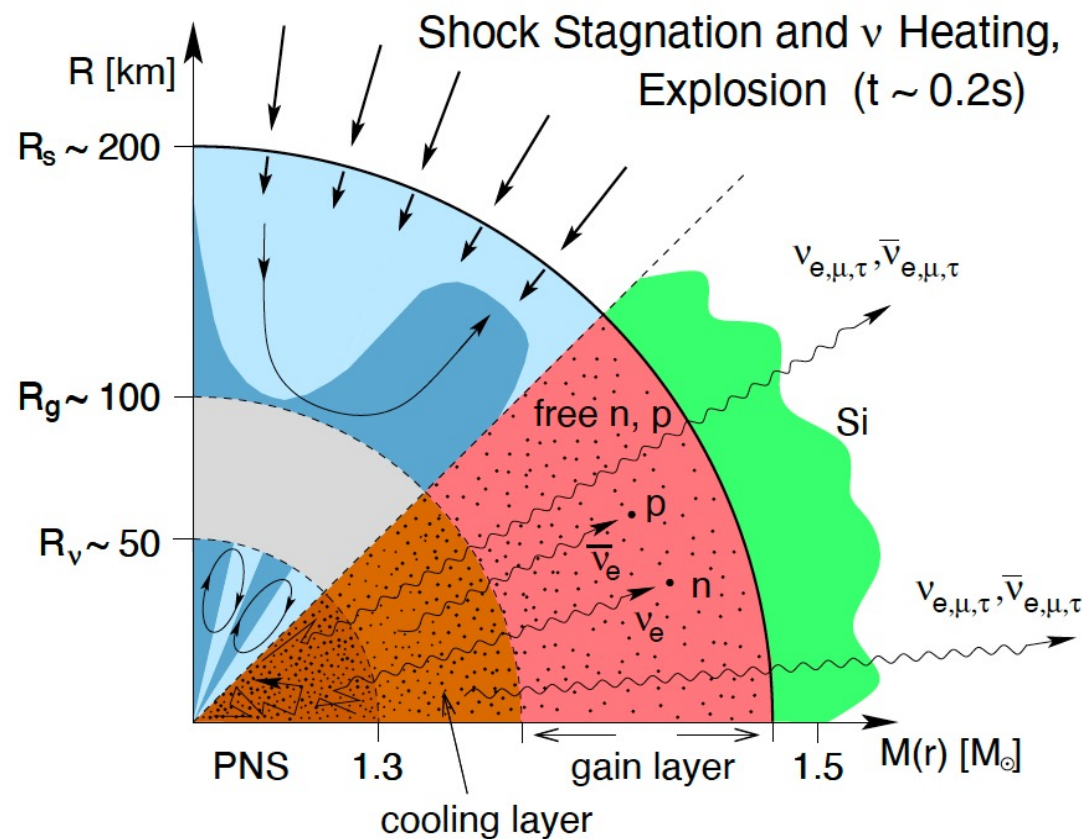
Formation of the PNS

➤ Neutrinos deposit energy behind the shock front:

- $\nu_e + n \rightarrow e^- + p$
- $\bar{\nu}_e + p \rightarrow e^+ + n$



ν -heating and "hot bubble"



Phases of collapse

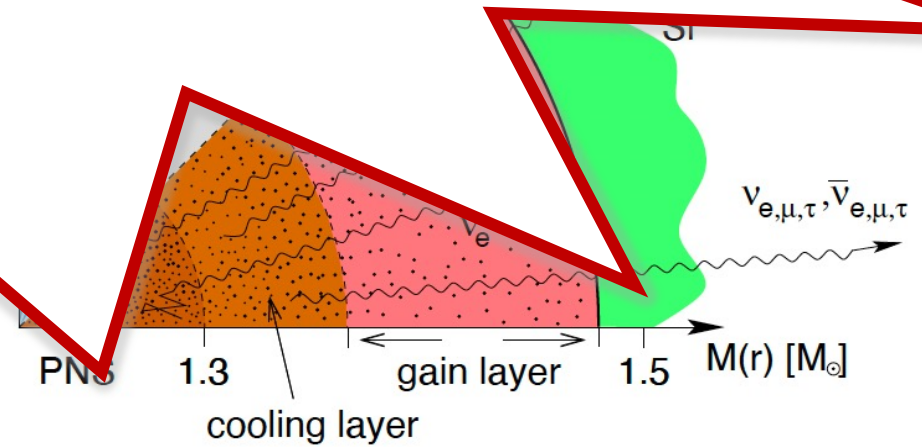
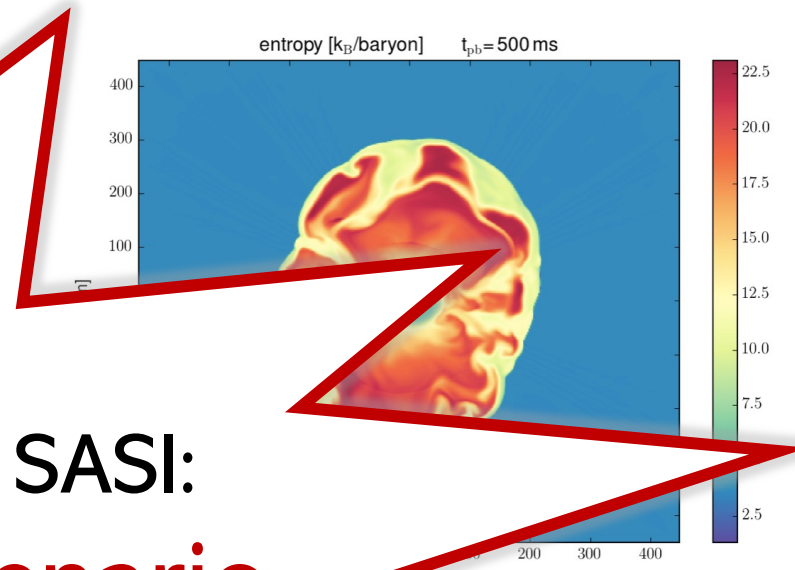
Neutrinos deposit energy in regions with low densities («Hot Bubbles»)

➤ At the **upper** end of the core, high pressure, low entropy

➤ At the **lower** end of the core, low pressure, high entropy

ν -heating + convection + SASI: Delayed Explosion Scenario

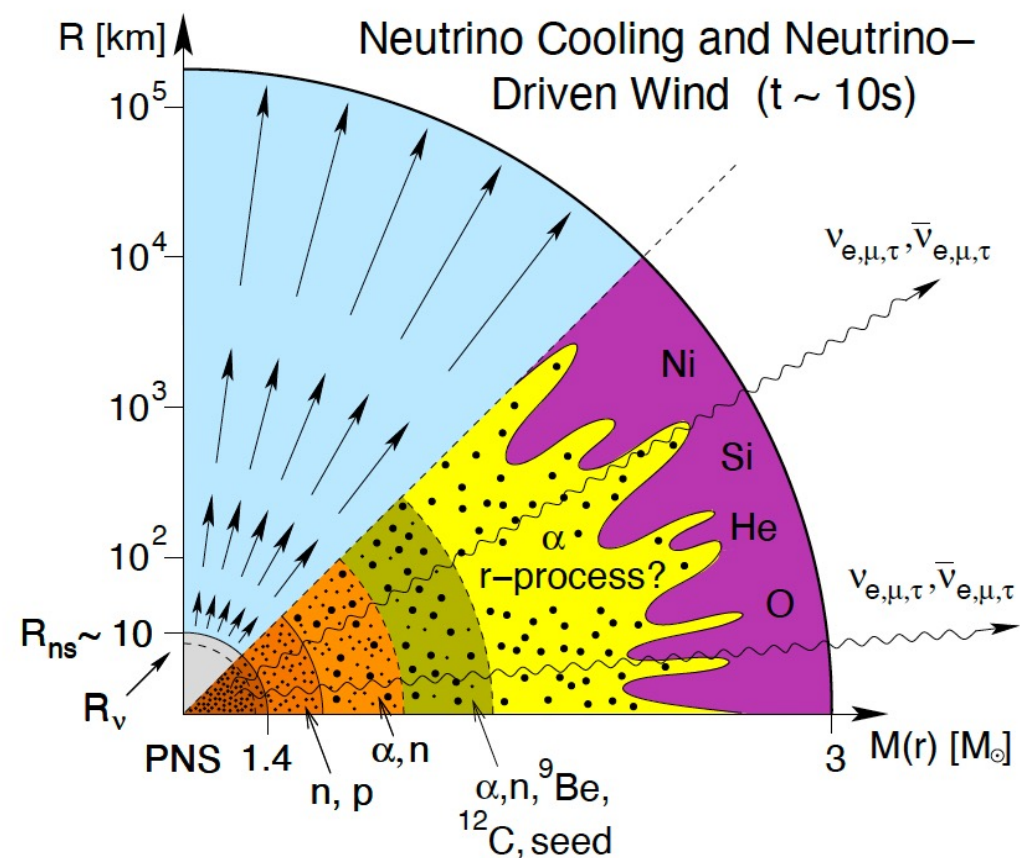
Post-shock convection and SASI
They help the shock revival



Phases of collapse

After the revival, the shock wave ejects all the SN mantle $E \sim 10^{51}$ erg.

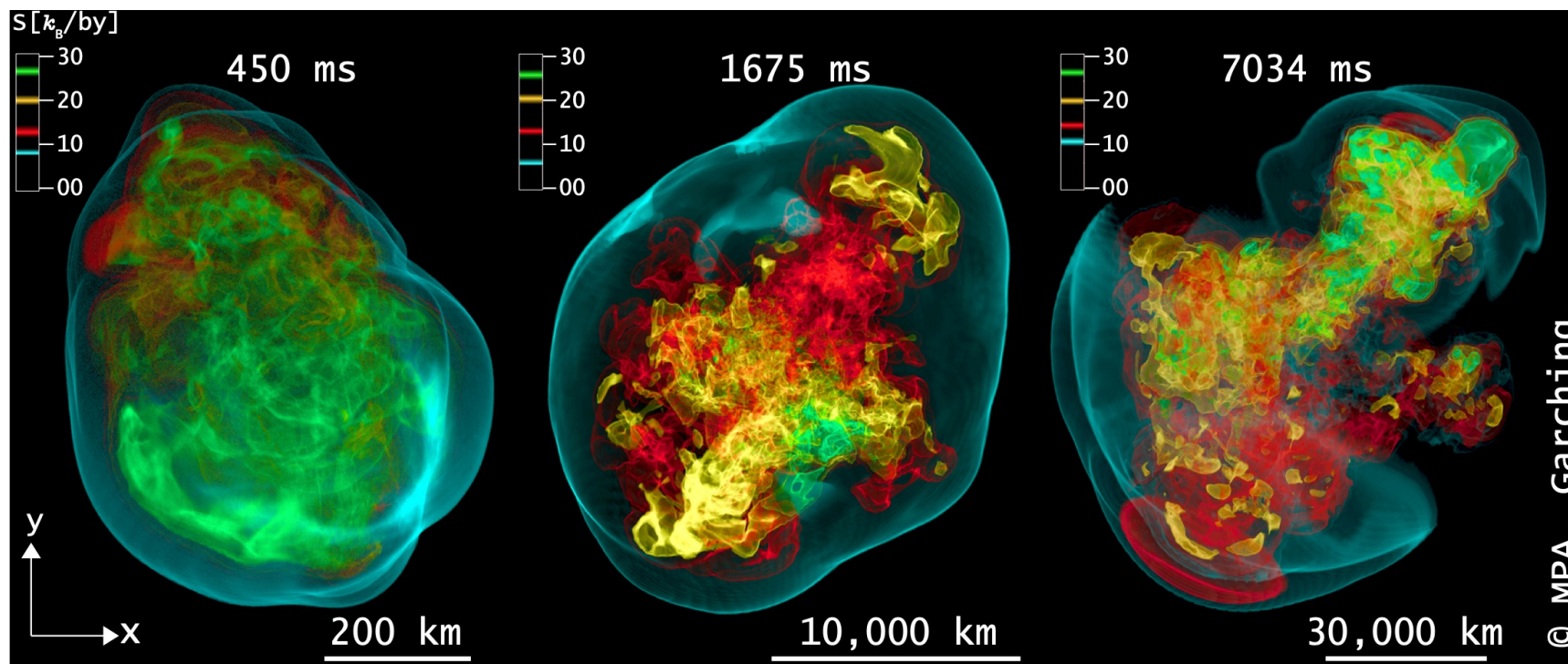
- Formation of a young Neutron Star at the centre ($R \sim 10$ km, $M \sim 1.5 M_{\odot}$).
- Cooling via neutrino emission of all species ($E \sim 10^{53}$ erg, $t \sim 10$ s).



Supernova simulations

Most of our knowledge about SN explosions is based on complex 3D simulations.

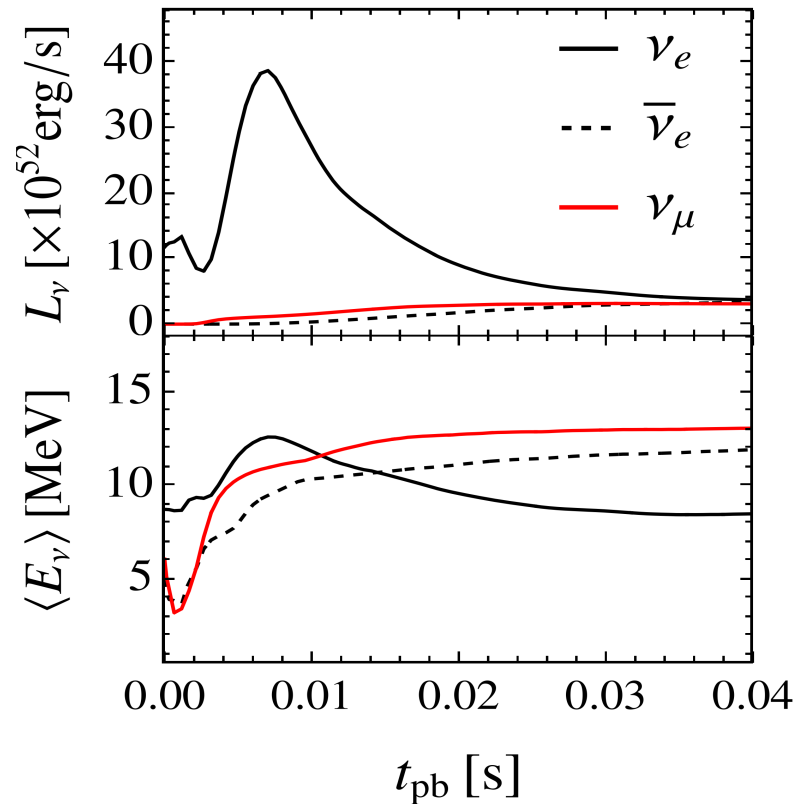
- Account for 3D neutrino transport equations
- Account for the effect of convection and SASI instabilities



Supernova neutrinos

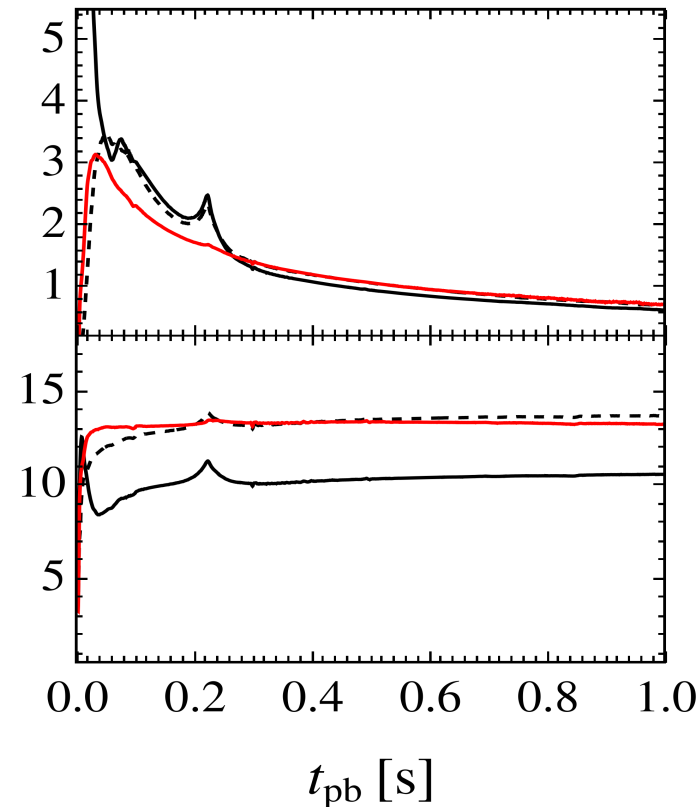
Neutronization burst

- Electron capture in the inner core



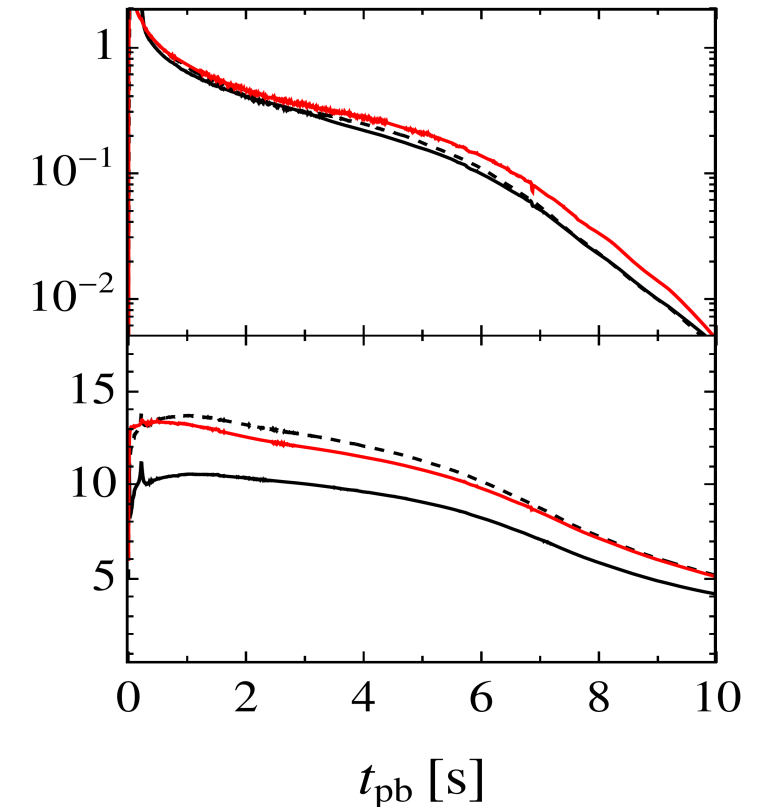
Accretion

- When shock stalls, ν powered by infalling matter

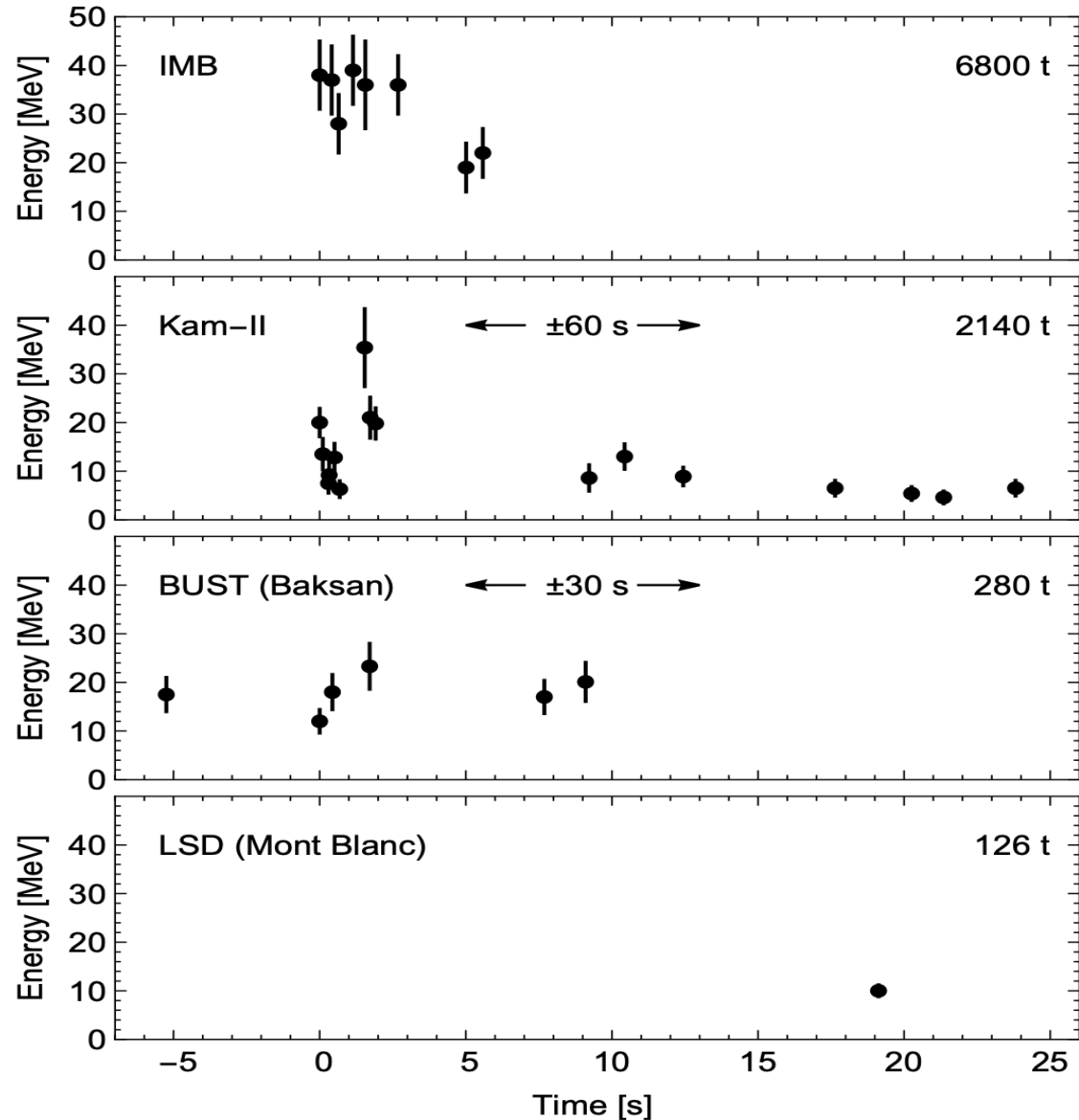


Cooling

- Cooling on ν diffusion time scale



SN 1987A



SN 1987A was the first and only SN event allowing for the observation of the associated neutrino burst so far.

➤ From SN 1987A neutrino burst observations:

- Duration of the burst ~ 10 s.
- $\langle E_\nu \rangle \approx 15$ MeV.

➤ Standard picture confirmed by SN 1987A observation.

Recent re-analysis showed that late time events are in tension with SN simulations.

[Fiorillo et al., Phys. Rev. D 108 (2023)]

ALP production in SNe

The QCD axion

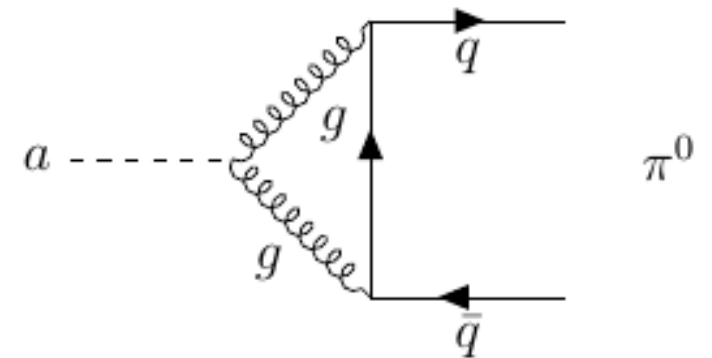
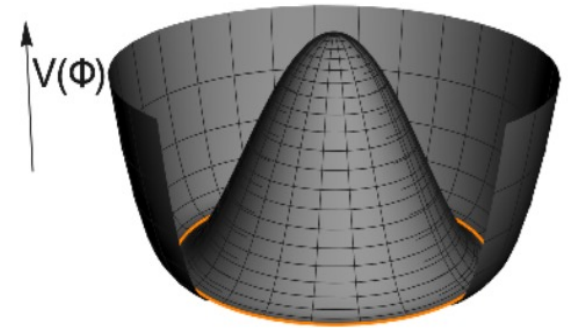
The *QCD axion* is a pseudoscalar particle postulated to solve the *Strong-CP problem* in QCD:

$$\mathcal{L}_{\text{CP}} = \theta \frac{\alpha_s}{8\pi} G_{\mu\nu}^a G^{\tilde{a}\mu\nu}$$

➔ PQ mechanism: global symmetry $U(1)_{\text{PQ}}$
spontaneously broken at f_a [*Peccei & Quinn, PRL 38 (1977)*]

The QCD axion acquires a small mass from its coupling to QCD.

$$m_a = 5.70(6)(4) \mu\text{eV} \left(\frac{10^{12} \text{GeV}}{f_a} \right)$$

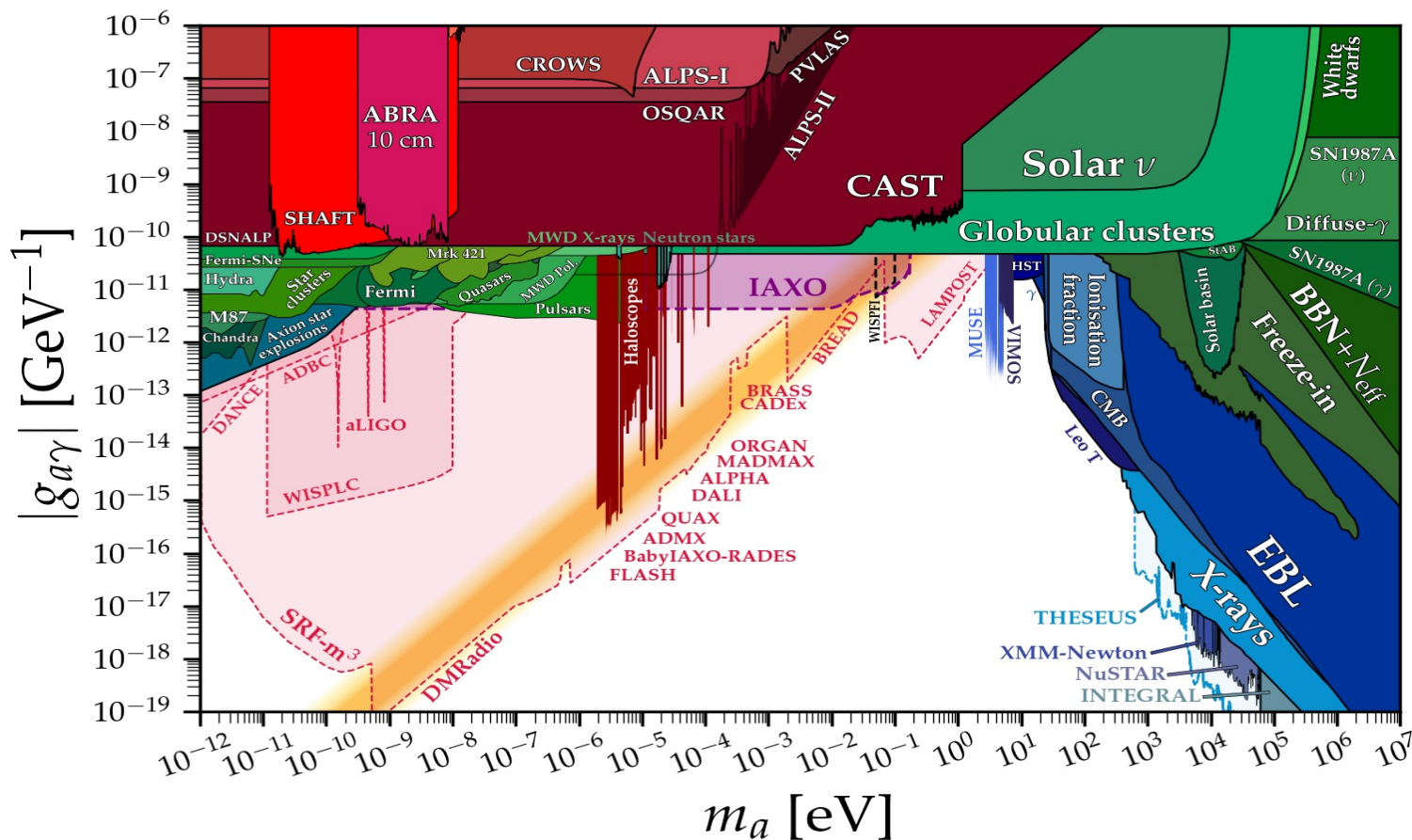


Axion-like particles

Many pseudoscalar particles behaving like the QCD axion emerge in UV extensions of Standard Model

- Vast landscape of axion-like particles (ALPs)
- No relation between ALP mass and couplings.

cajohare.github.io/AxionLimits/



ALP nuclear interactions

- Axions and ALPs could interact with all the Standard model particles.

$$\mathcal{L}_a \supset \frac{\alpha_s}{8\pi} \frac{C_g}{f_a} a G_{\mu\nu}^a \tilde{G}^{a\mu\nu} - \frac{1}{4} g_{a\gamma} a F_{\mu\nu} \tilde{F}^{\mu\nu} - \sum_{\psi} \frac{g_{a\psi}}{2m_{\psi}} \bar{\psi} \gamma_{\mu} \gamma_5 \psi \partial^{\mu} a$$

- In ChPT interaction vertices with baryons and mesons [*Ho & al., Phys. Rev. D 107 (2023)*]

$$\begin{aligned} \mathcal{L}_{\text{int}} = & g_a \frac{\partial_{\mu} a}{2m_N} \left[C_{ap} \bar{p} \gamma^{\mu} \gamma_5 p + C_{an} \bar{n} \gamma^{\mu} \gamma_5 n + \right. \\ & + \frac{C_{a\pi N}}{f_{\pi}} (i\pi^+ \bar{p} \gamma^{\mu} n - i\pi^- \bar{n} \gamma^{\mu} p) + \\ & \left. + C_{aN\Delta} \left(\bar{p} \Delta_{\mu}^+ + \overline{\Delta_{\mu}^+} p + \bar{n} \Delta_{\mu}^0 + \overline{\Delta_{\mu}^0} n \right) \right] \end{aligned}$$

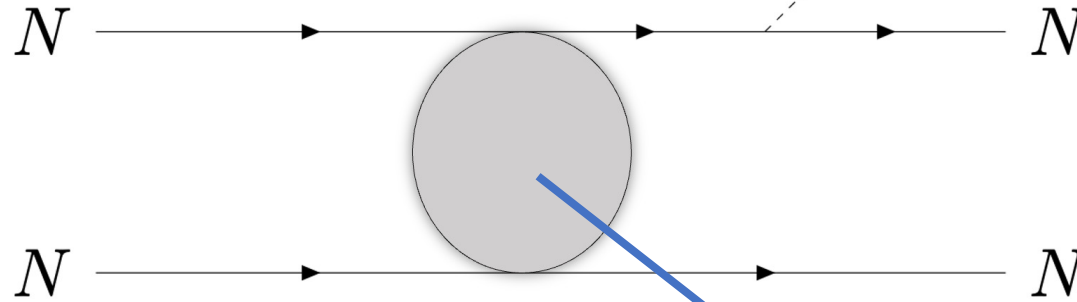
ALP production in SNe

➤ Nucleon-Nucleon bremsstrahlung

[Carenza & al., JCAP 10 (2019) 10,
Raffelt & Seckel, Phys. Rev. D 52 (1995),
Hempel, Phys. Rev. C 91 (2015),
Ericson and Mathiot, Phys. Lett. B 219 (1989)]

Effective nucleon masses

$$m_N \rightarrow m_N^*$$

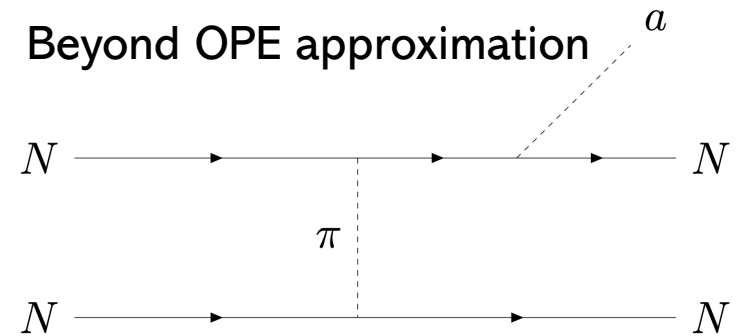


$$a \longrightarrow m_a \neq 0$$

AL & al., Phys. Rev. D 107 (2023)

Nucleons multiple scattering

$$S_\sigma = \frac{\Gamma_\sigma}{\omega^2 + \Gamma^2} s_\sigma$$

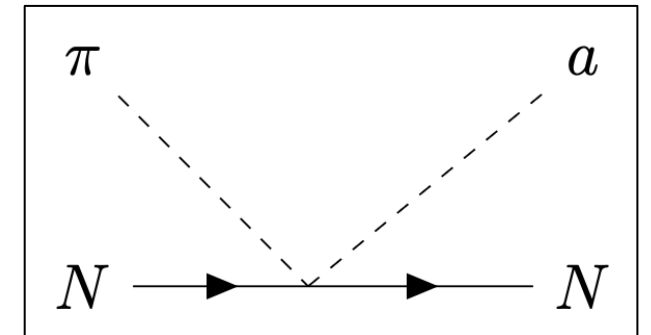
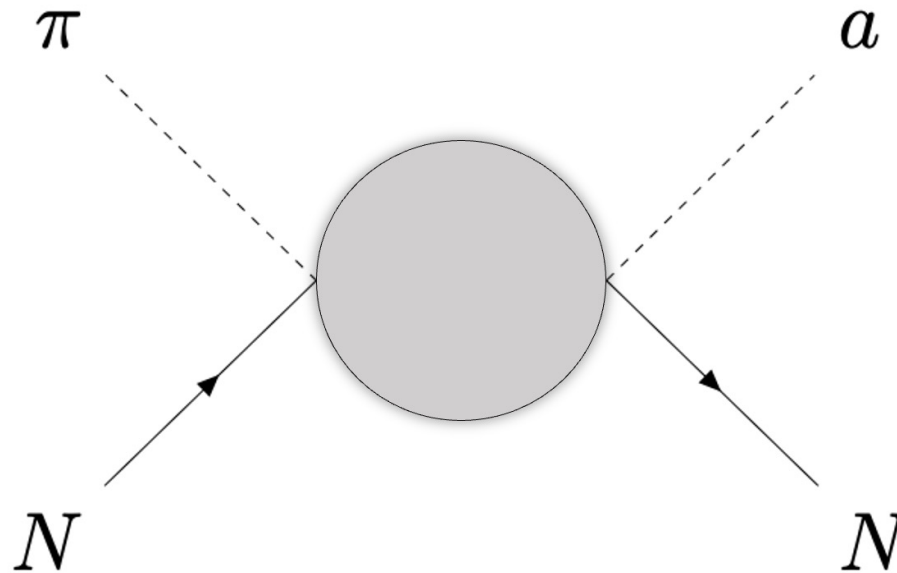
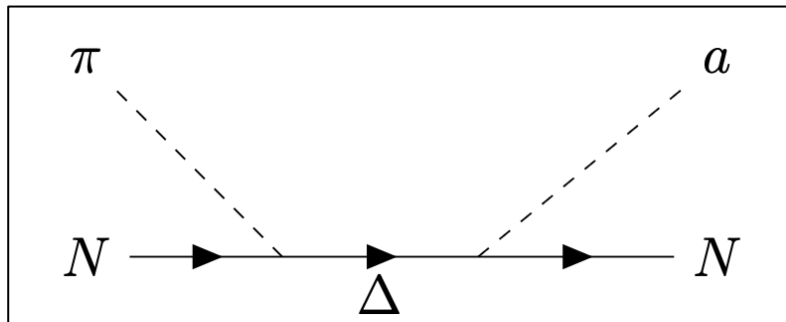
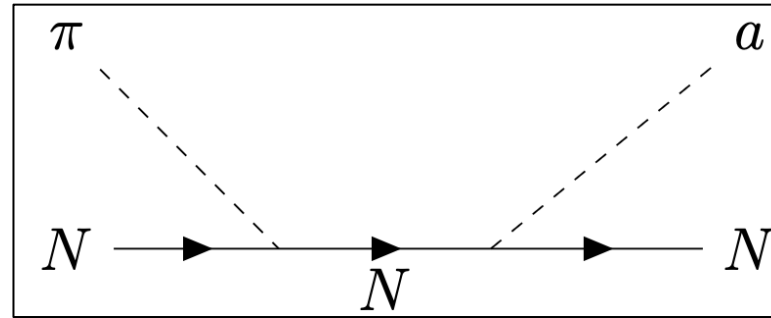


Beyond OPE approximation

ALP production in SNe

➤ Pion Conversions

[Carenza & al., *Phys.Rev.Lett.* 126 (2021),
Choi & al., *JHEP* 02 (2022) 143,
Ho & al., *Phys. Rev. D* 107 (2023)]



ALP emission spectra

- If ALPs interact weakly with nuclear matter, they can *free-stream* through the SN volume

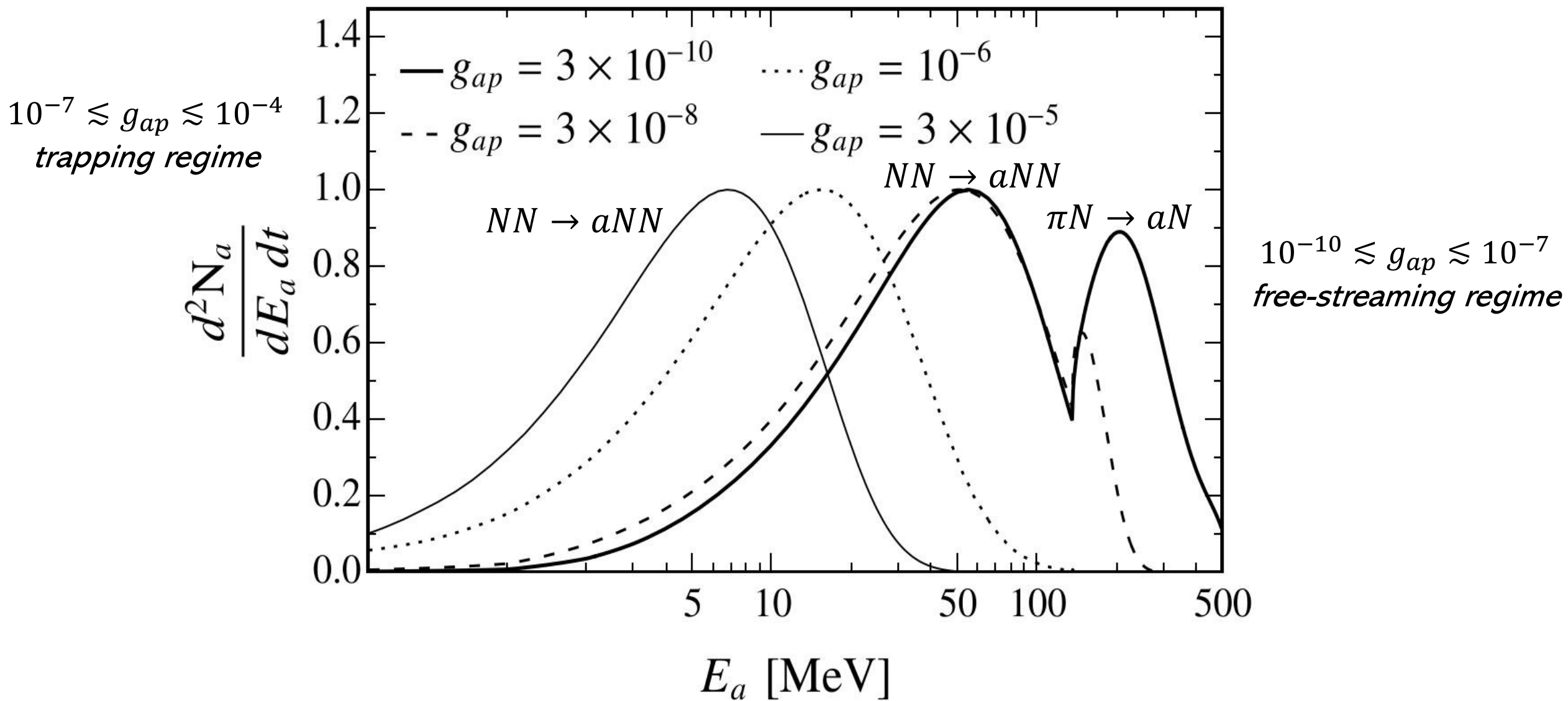
$$\frac{d^2 N_a}{dE_a dt} = \int_0^\infty 4\pi r^2 dr \frac{d^2 n_a}{dE_a dt}$$

- In case of strongly coupled ALPs, they could enter the *trapping regime*
[Caputo & al., Phys. Rev. D 105 (2022)]

$$\frac{d^2 N_a}{dE_a dt} = \int_0^\infty 4\pi r^2 dr \left\langle e^{-\tau(E_a, r)} \right\rangle \frac{d^2 n_a}{dE_a dt}$$

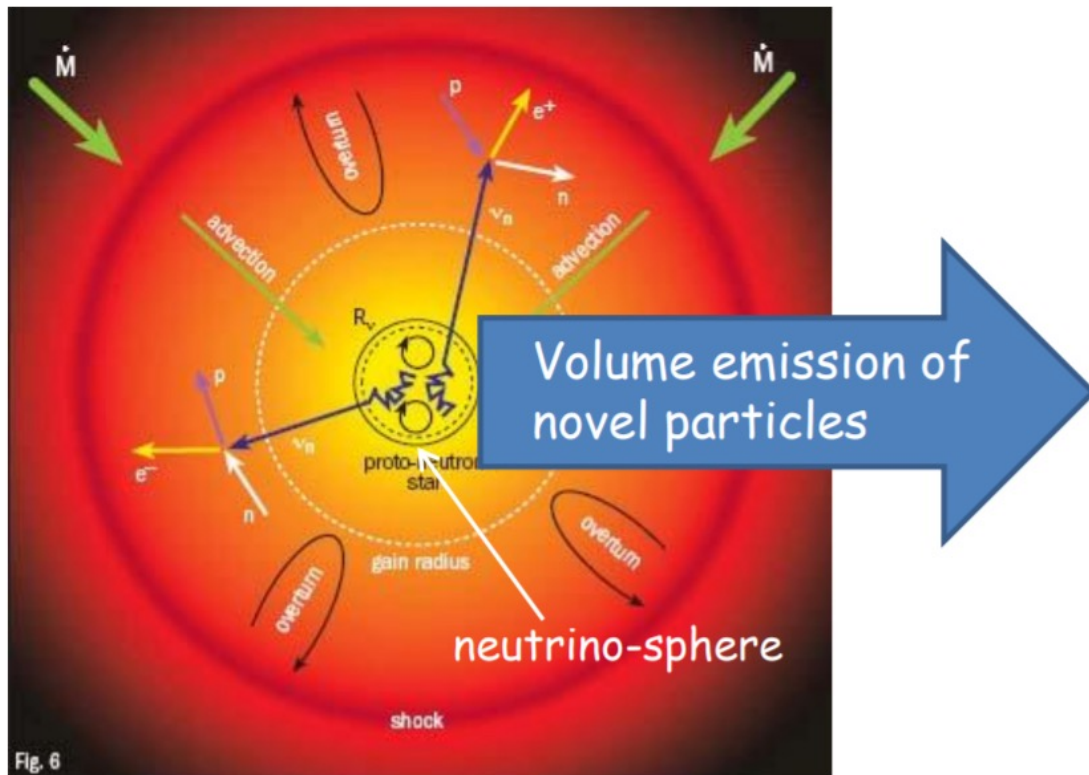
$$\tau \sim \int_0^\infty dr \lambda_a^{-1} \text{ optical depth for nuclear processes}$$


ALP emission spectra



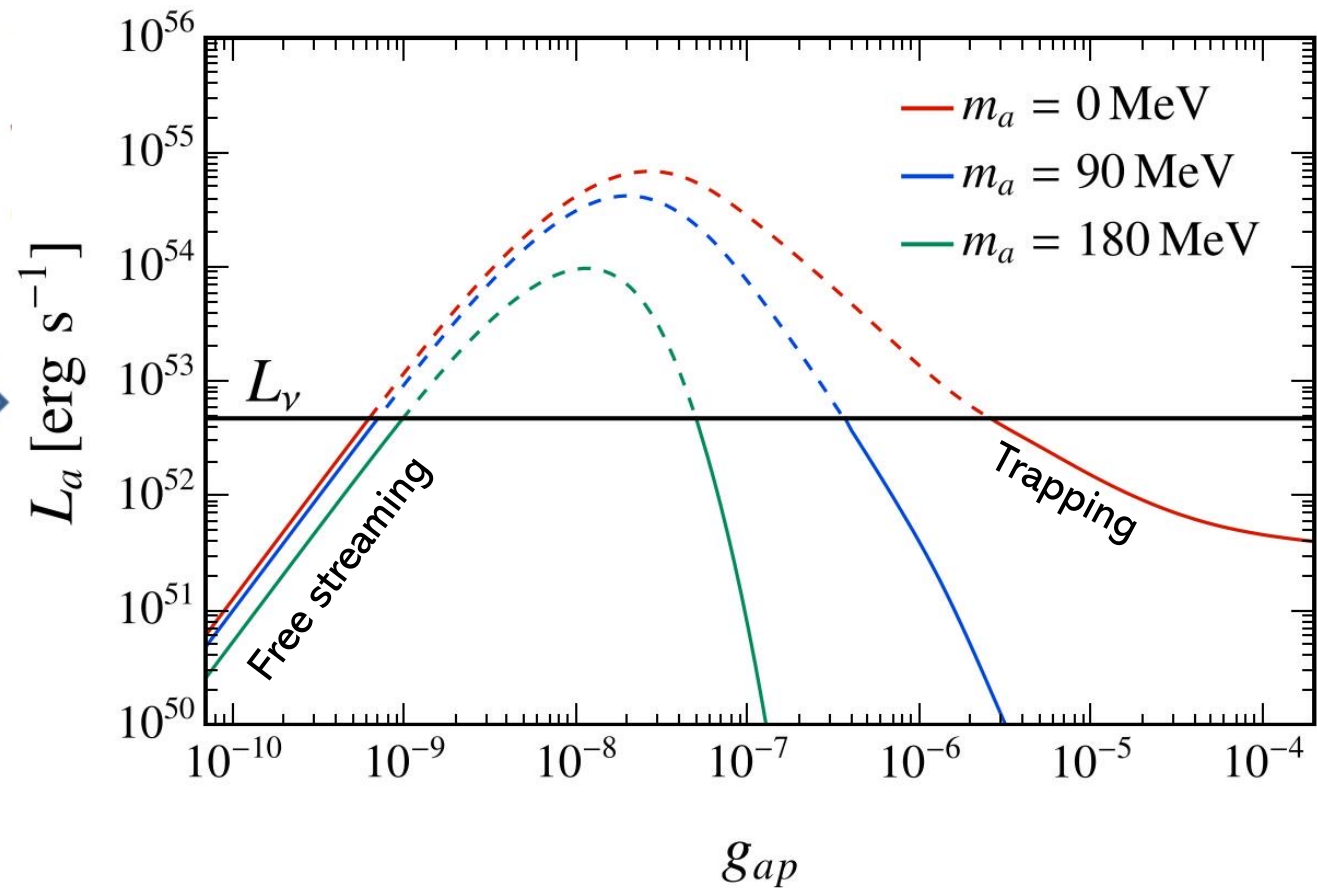
The energy-loss argument

Emission of exotic particles could cause an excessive energy-loss from SNe, affecting the neutrino burst.



[Raffelt & Seckel, Phys. Rev. Lett. 60 (1998)]

[AL & al., Phys. Rev. D 109 (2024) 2]



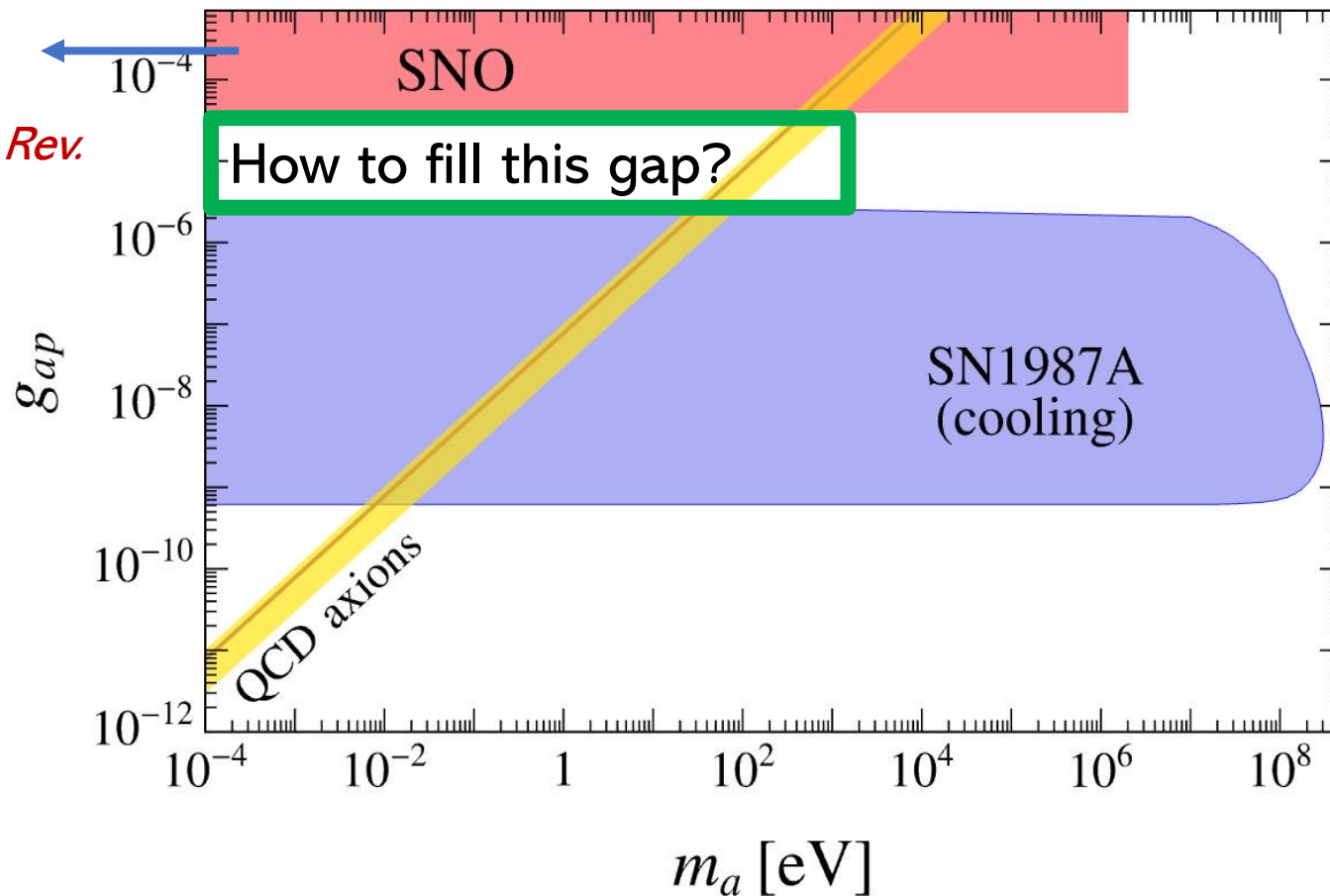
The energy-loss argument

Assuming that ALP emission did not shorten the duration of the neutrino burst more than $\sim 1/2$, we require that [*Raffelt, Phys. Rept. 198 (1990)*]:

$$L_a \lesssim L_\nu \quad \text{at } t_{\text{pb}} = 1 \text{ s}$$

Searches for solar axions in SNO.

[*Bhusal et al., Phys. Rev. Lett. 126 (2021)*]



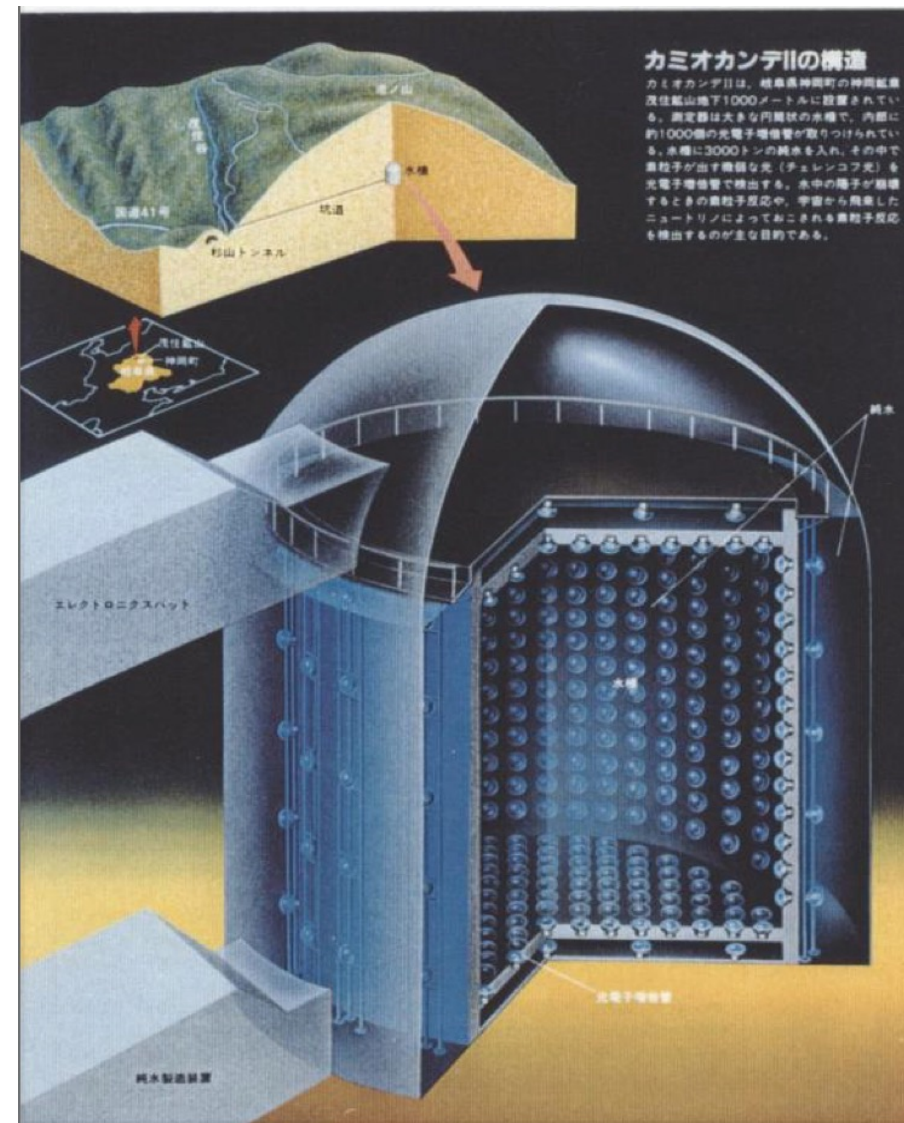
[*AL & al., Phys. Rev. D 109 (2024) 2*]

Axion signal in Kamiokande-II

- In case of strong couplings the ALP flux would have produced a signal in Kamiokande II.
- Seminal idea by Engel, Seckel and Hayes: look for axion-induced excitation of oxygen nuclei [*Engel et al., Phys. Rev. Lett. 65 (1990)*].



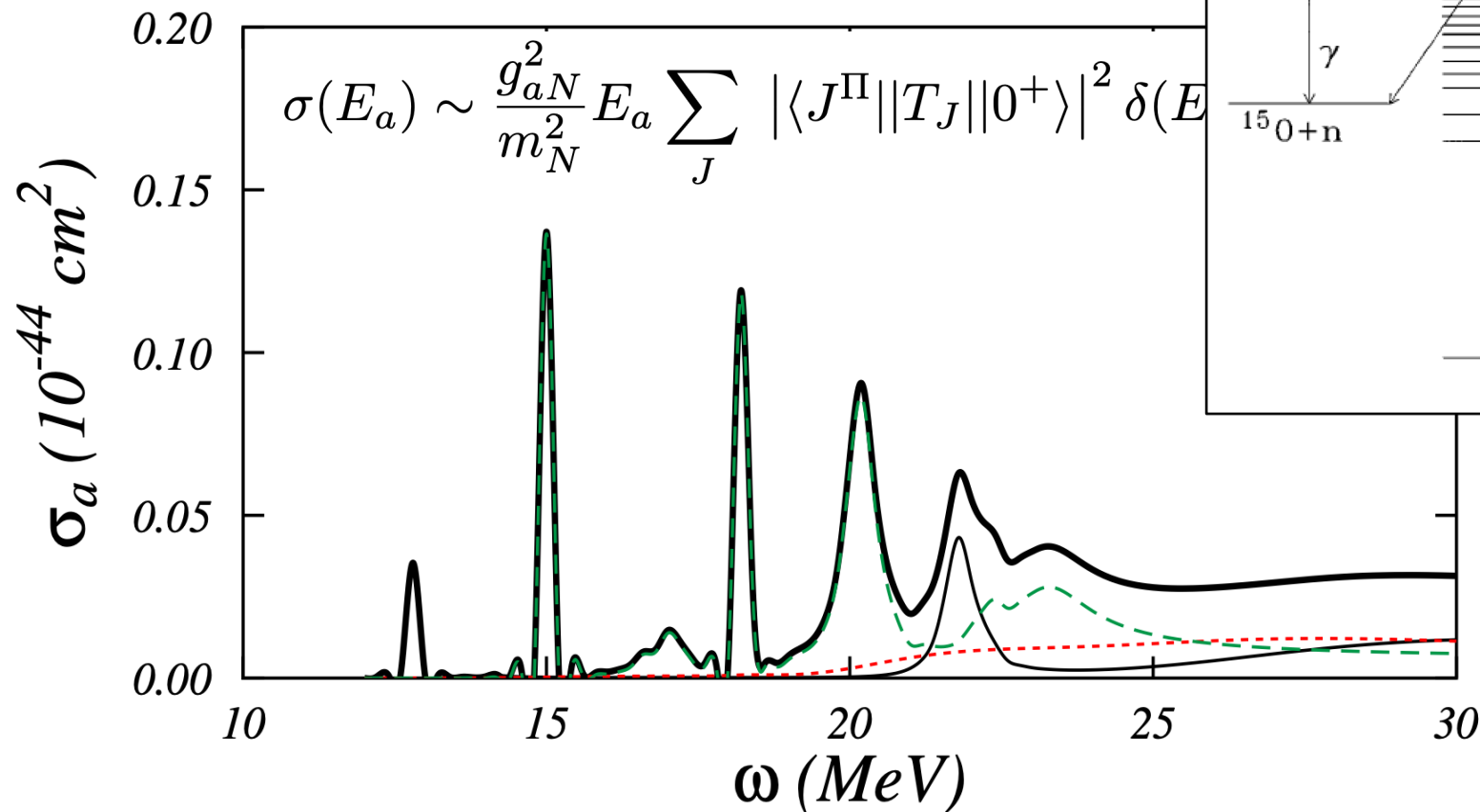
- The computation of the event rate requires:
 - SN explosion models
 - An adequate treatment of trapping regime
 - State-of-the-art nuclear models



Axion-oxygen cross section

Introducing $C_0 = (C_p + C_n)/2$ and $C_1 = (C_p - C_n)/2$, Axion-nucleons interactions reads

$$\mathcal{H}_{aN} = -\frac{g_{aN}}{2m_N} \partial_k a \underbrace{\bar{N} \gamma^k \gamma^5 (C_0 + C_1 \tau_3)}_{\text{Hadronic current}}$$



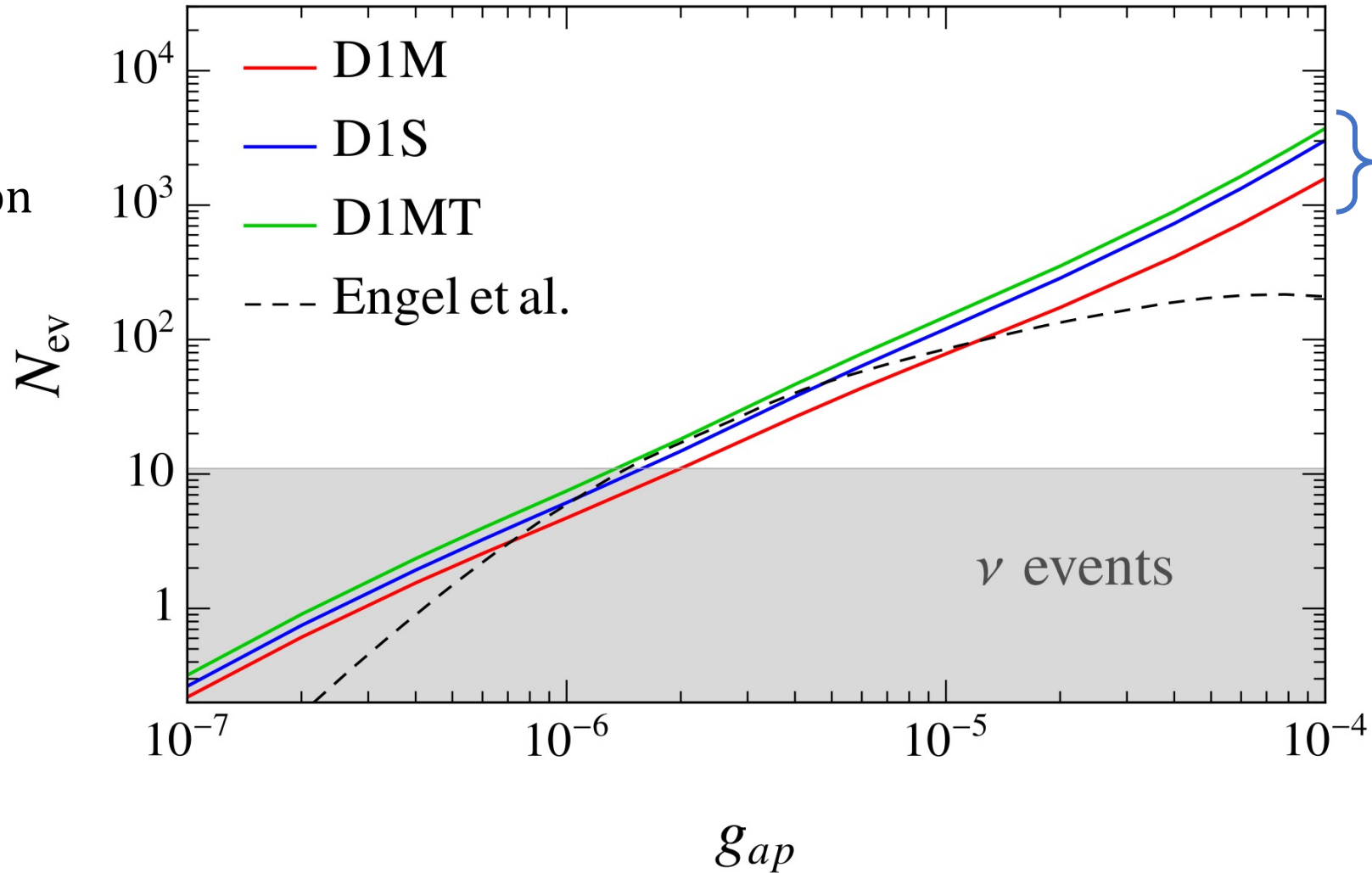
$$\sigma(E_a) \sim \frac{g_{aN}^2}{m_N^2} E_a \sum_J |\langle J^\Pi || T_J || 0^+ \rangle|^2 \delta(E_a - E_J)$$

[P. Carenza, G. Co',
M. Giannotti, AL, G. Lucente,
A. Mirizzi, T. Rauscher,
Phys. Rev. C 109 (2024) 1]

Events number in Kamiokande-II

$$N_{\text{ev}} = F_a \otimes \sigma \otimes \mathcal{R} \otimes \mathcal{E}$$

$M_{KII} \sim 2.4 \text{ kton}$

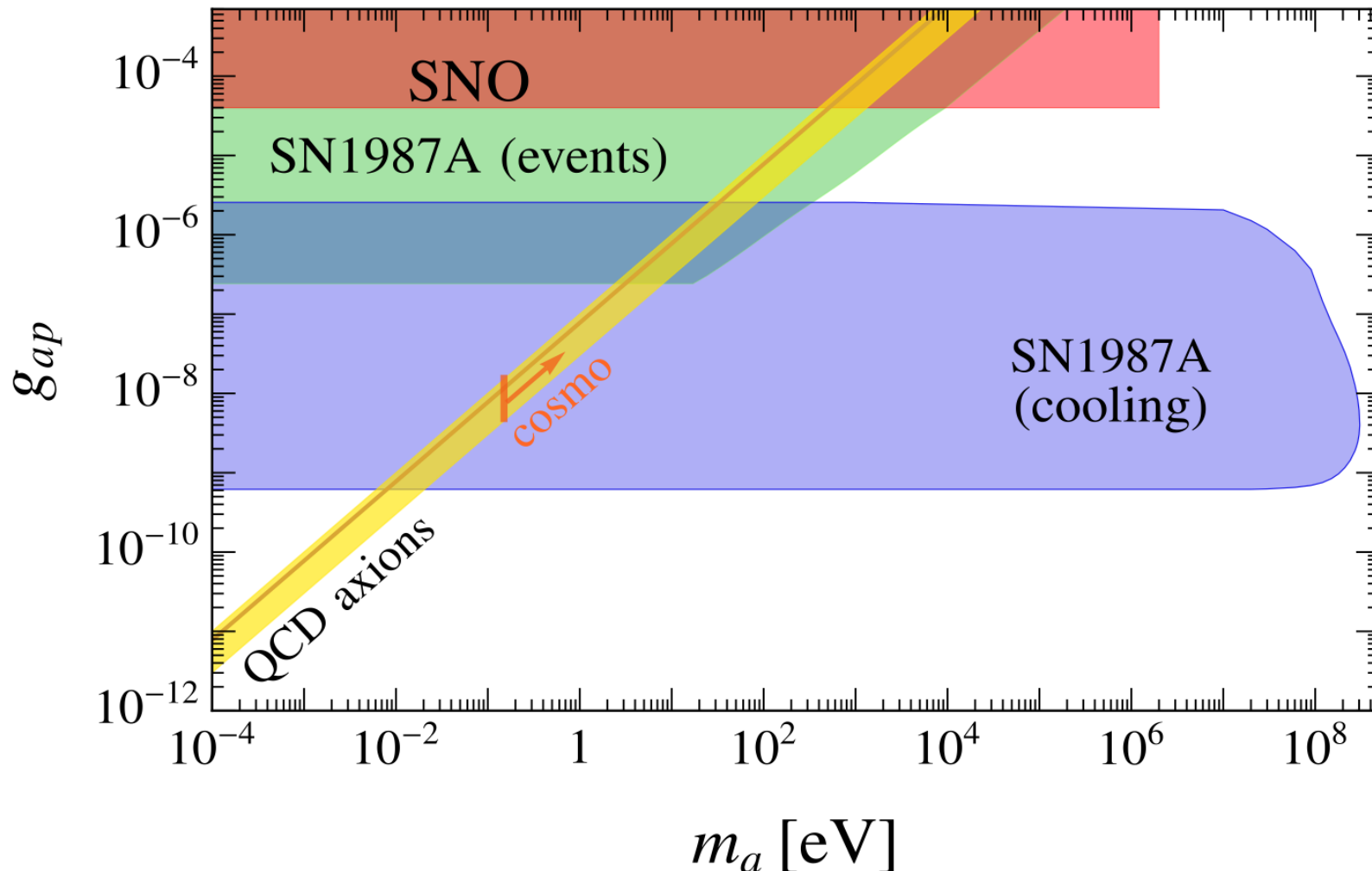


Uncertainties
 $\mathcal{O}(60\%)$ over the
nuclear model

Axion events from SN 1987A

No excess in the background of K-II around SN 1987A event ($\bar{n}_{bkg} \simeq 0.02$ events/s)

[*Kamiokande Coll., Phys. Rev. Lett. 58 (1987) 1490*].



[*AL & al.,
Phys. Rev. D 109 (2024) 2*]

[*P. Carenza, G. Co', M. Giannotti, AL, G.
Lucente, A. Mirizzi, T. Rauscher,
Phys. Rev. C 109 (2024) 1*]

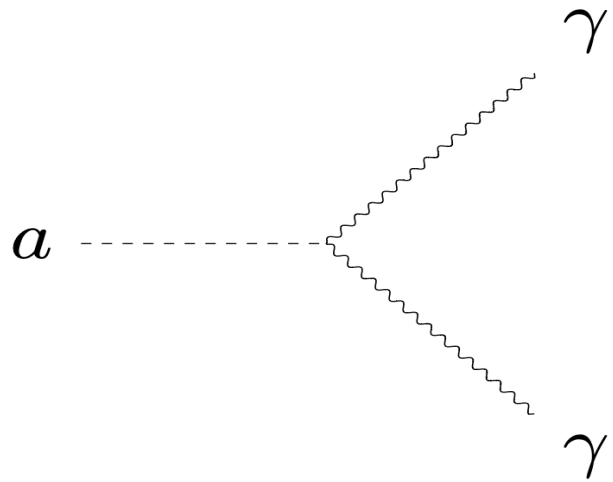
Observable signatures from decays

$$[m_a \sim \mathcal{O}(10)MeV]$$

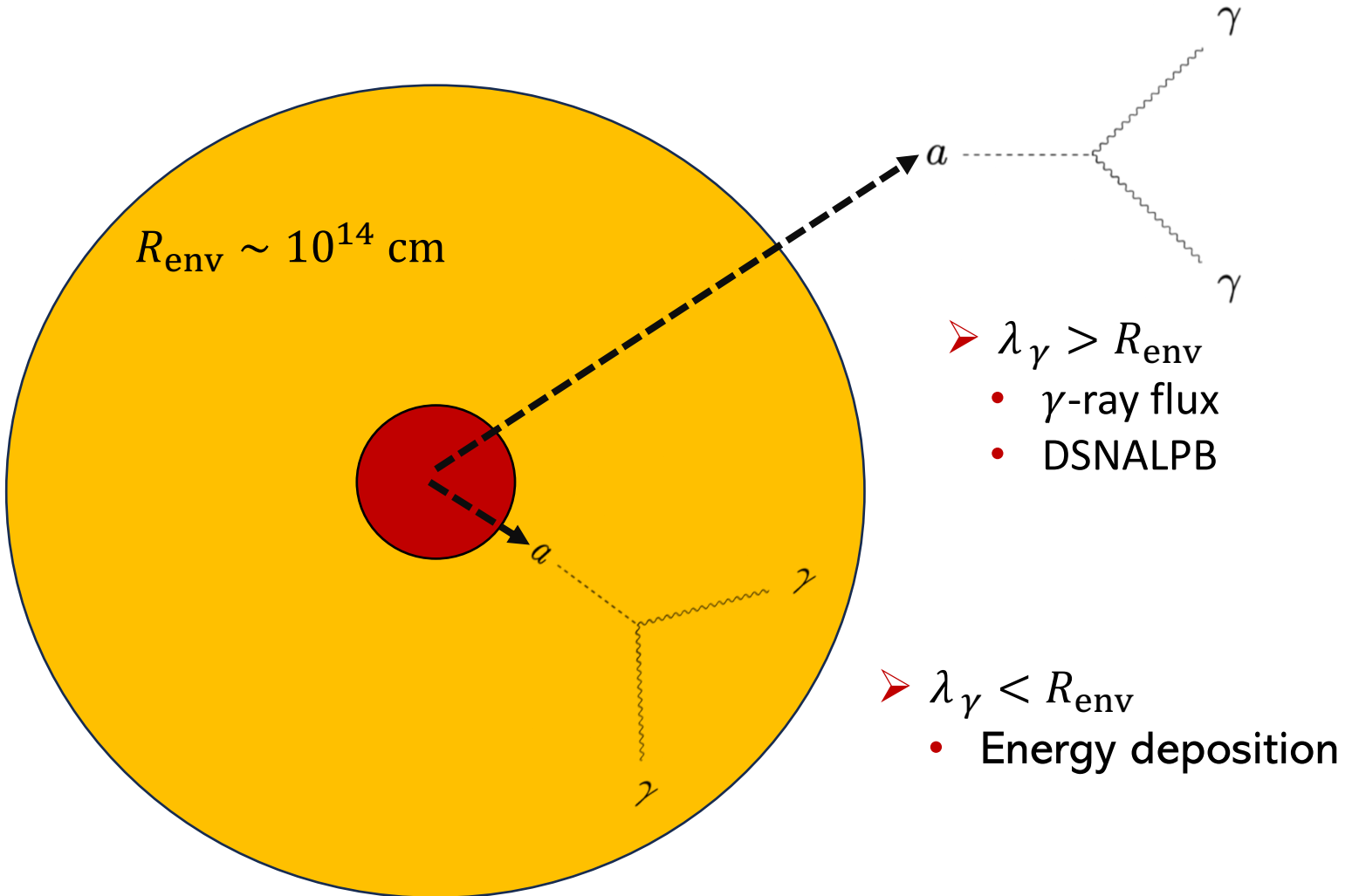
ALP decays

After being produced in the core, massive ALPs could decay into photon pairs.

$$\mathcal{L}_{a\gamma} = -\frac{1}{4}g_{a\gamma}F_{\mu\nu}\tilde{F}^{\mu\nu}a$$

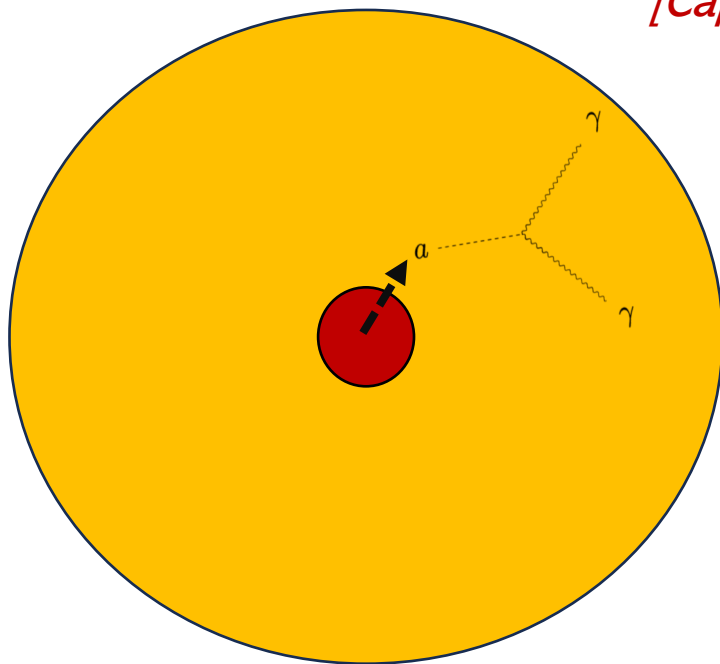


$$\Gamma_{a\gamma\gamma} = g_{a\gamma}^2 \frac{m_a^3}{64\pi}$$



Energy deposition

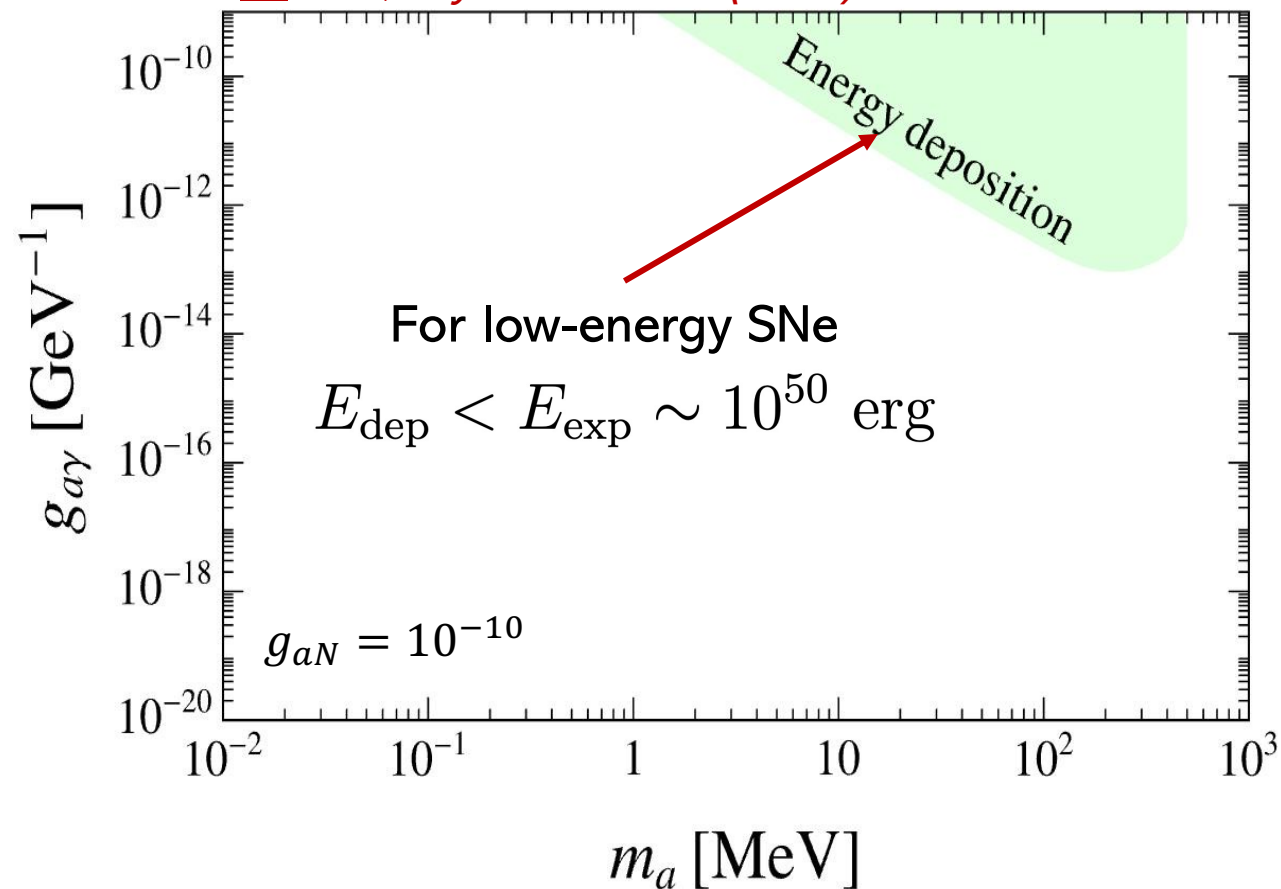
[Caputo et al., Phys. Rev. Lett. 128 (2022)]



ALPs decaying inside the SN envelope would deposit energy in the mantle

$$E_{\text{dep}} = \int dt \int_0^{R_{\text{PNS}}} dr 4\pi r^2 \int_0^\infty d\omega_a \omega_a \frac{dn_a}{d\omega_a dt} \times \left[e^{-(R_{\text{PNS}}-r)/\lambda_\gamma} - e^{-(R_{\text{env}}-r)/\lambda_\gamma} \right]$$

AL & al., Phys. Rev. D 107 (2023)



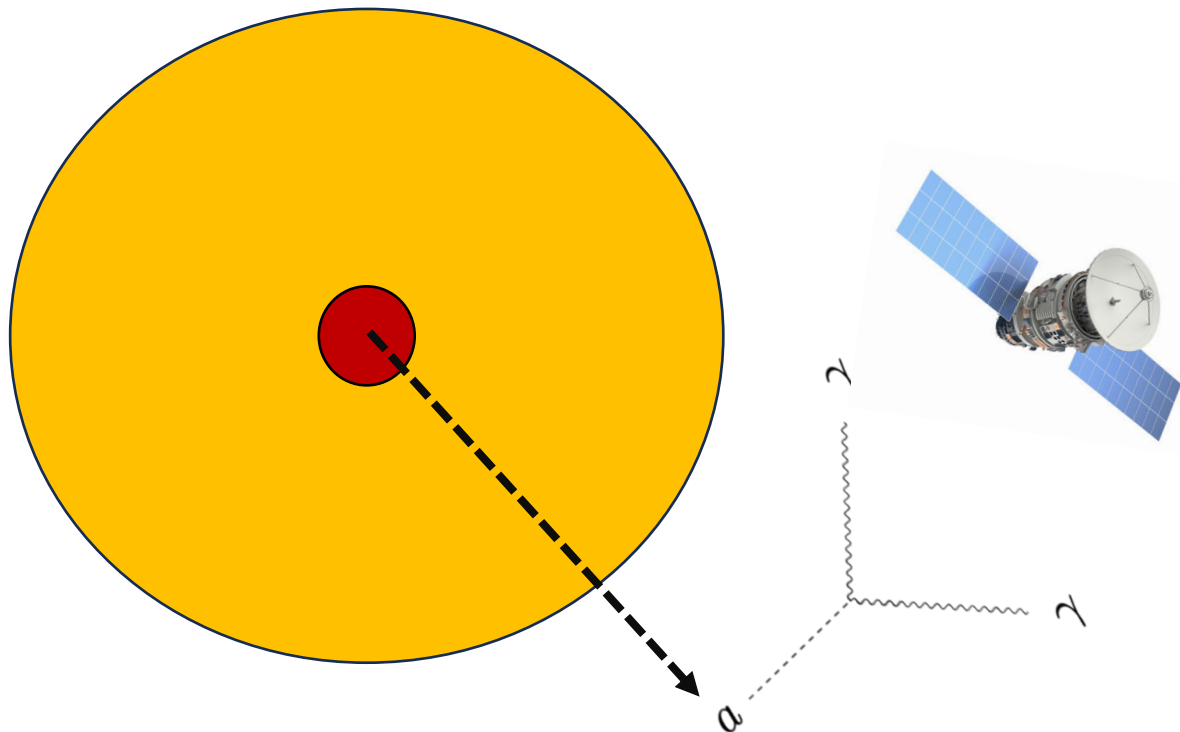
γ -ray bursts from SNe

[Jaeckel et al., Phys. Rev. D 98 (2018)]

[Hoof & Schulz, JCAP 03 (2023) 054]

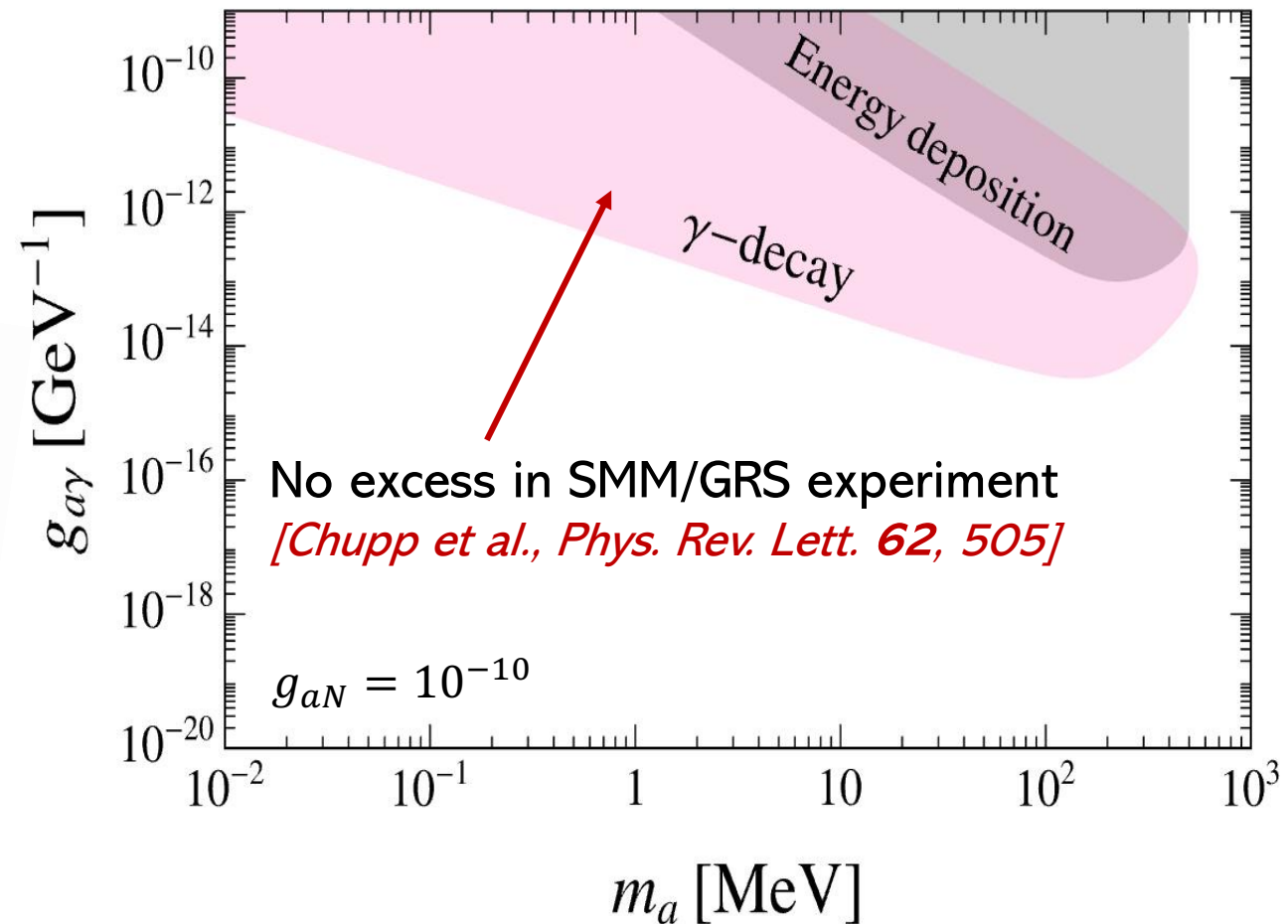
[Ravensburg et al., JCAP 07 (2023) 056]

ALPs decaying outside the SN envelope produce an additional photon flux



Alessandro Lella

AL & al., Phys. Rev. D 107 (2023)



Frascati, 29/07/2025

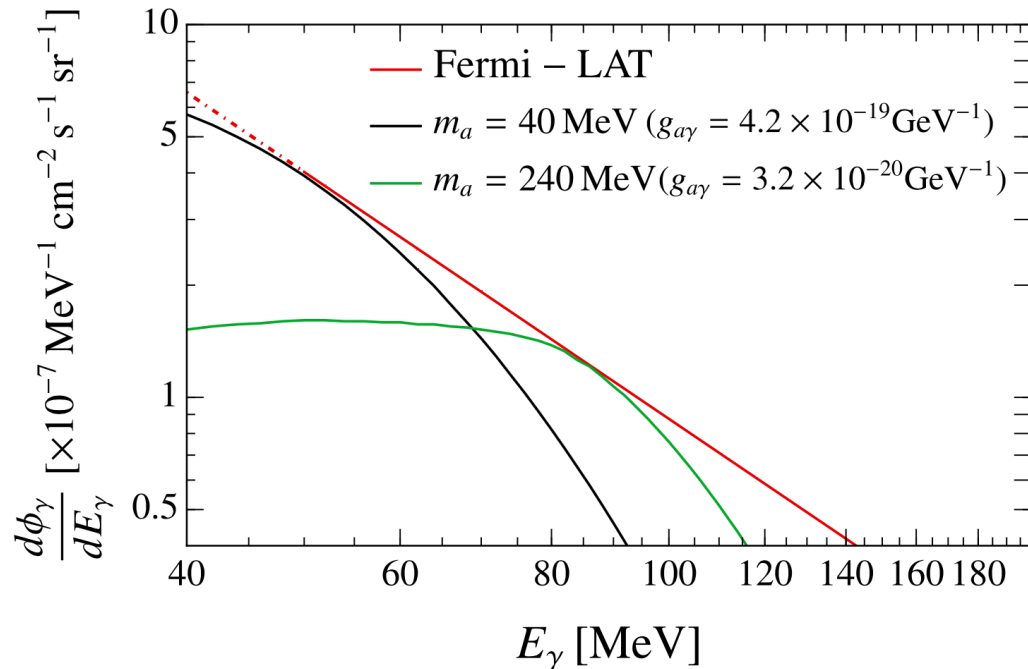
DSNALPB

[Beacom et al., *Ann. Rev. Nucl. Part. Sci.* 60 (2010)]

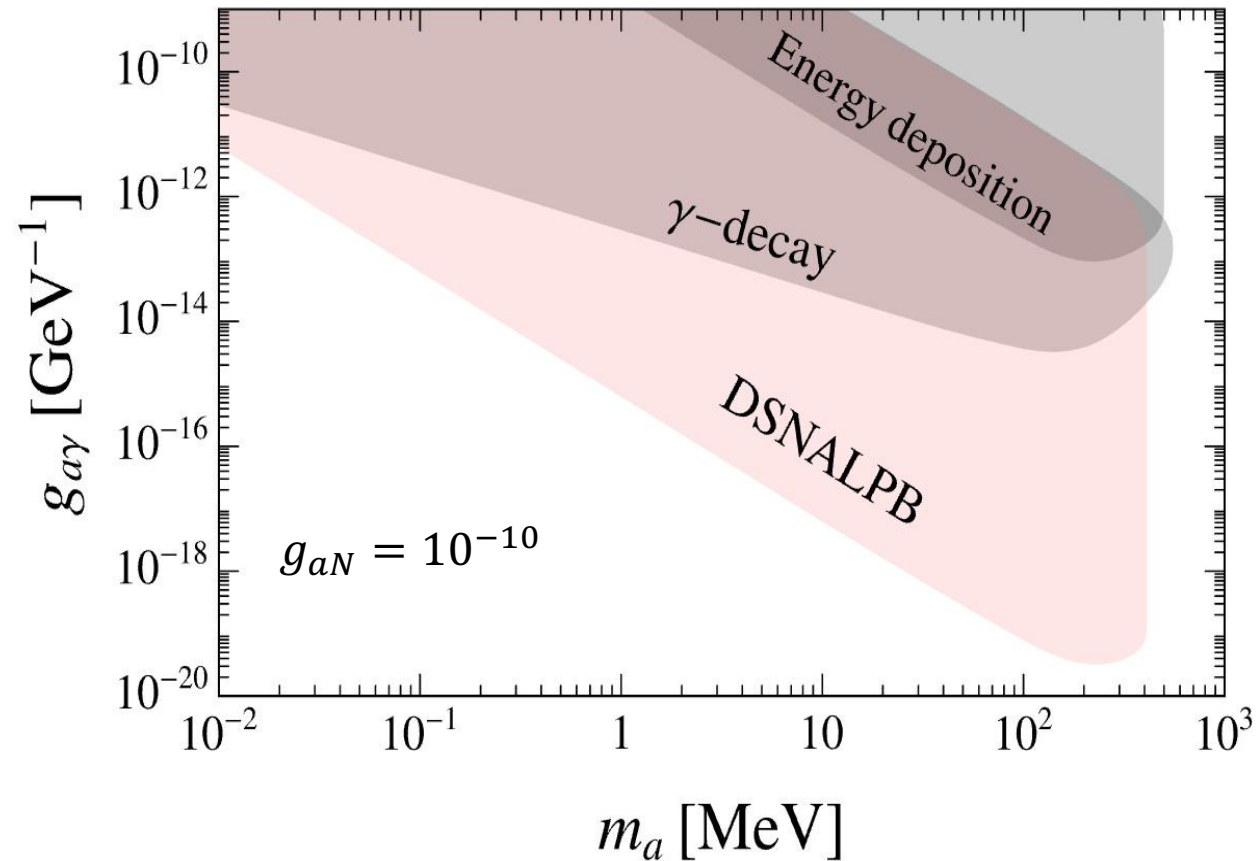
[Calore et al., *Phys. Rev. D* 102 (2020)]

ALPs emitted during all the past SN explosion could have given rise to a diffuse ALP background

$$\frac{d\phi_\gamma^{\text{dif}}}{dE_\gamma} = \int_0^\infty (1+z) \frac{dN_\gamma(E_\gamma(1+z))}{dE_\gamma} [R_{SN}(z)] \left[\left| \frac{dt}{dz} \right| dz \right]$$



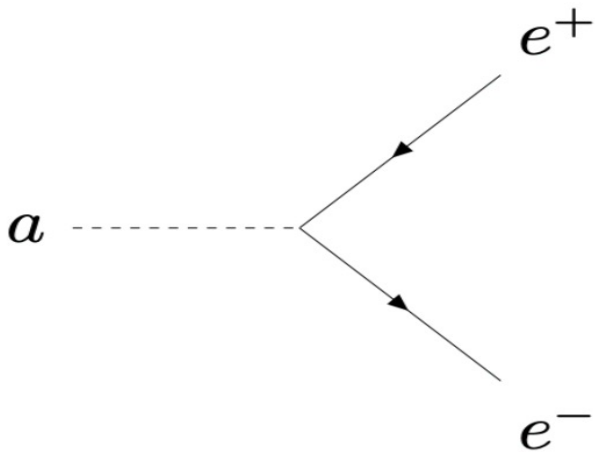
AL & al., Phys. Rev. D 107 (2023)



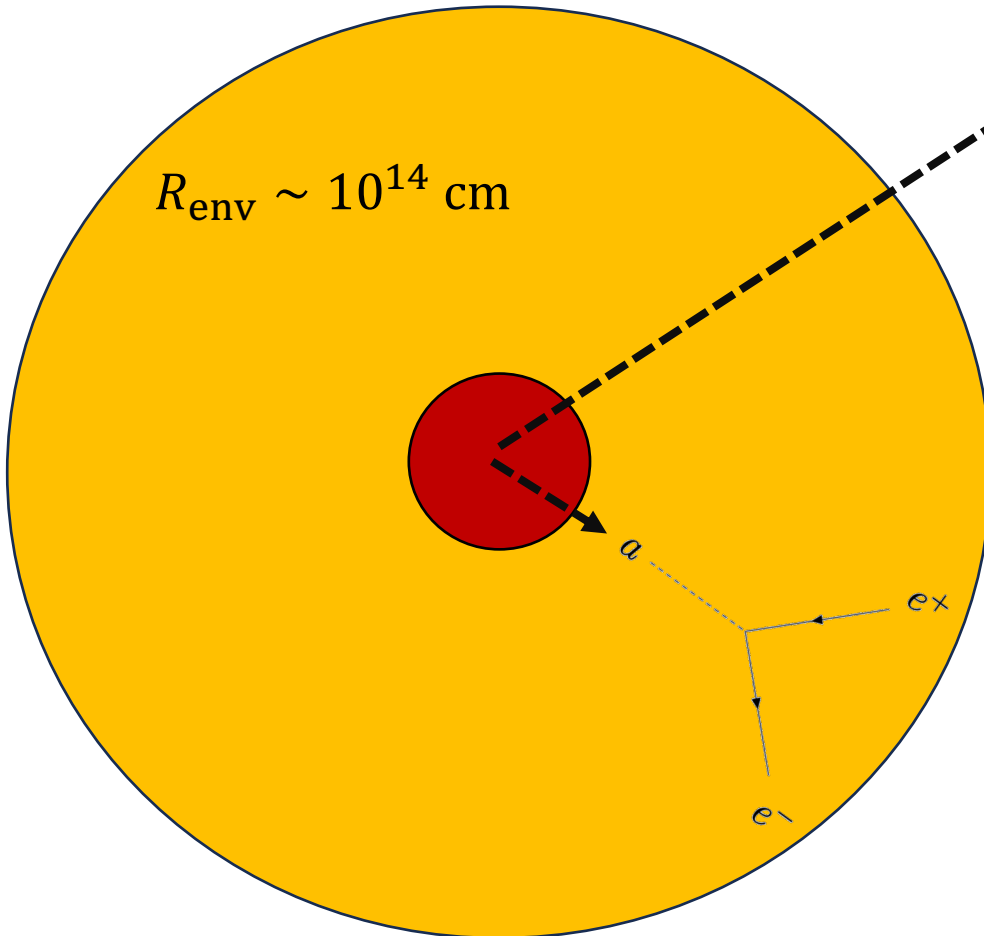
ALP decays

After being produced in the core, massive ALPs could decay into lepton pairs.

$$\mathcal{L}_{ae} = \frac{g_{ae}}{2m_e} (\bar{e}\gamma_\mu\gamma_5 e)\partial^\mu a$$



$$\lambda_e = \frac{8\pi}{g_{ae}^2 m_a} \sqrt{\frac{E_a^2 - m_a^2}{m_a^2 - 4m_e^2}}$$



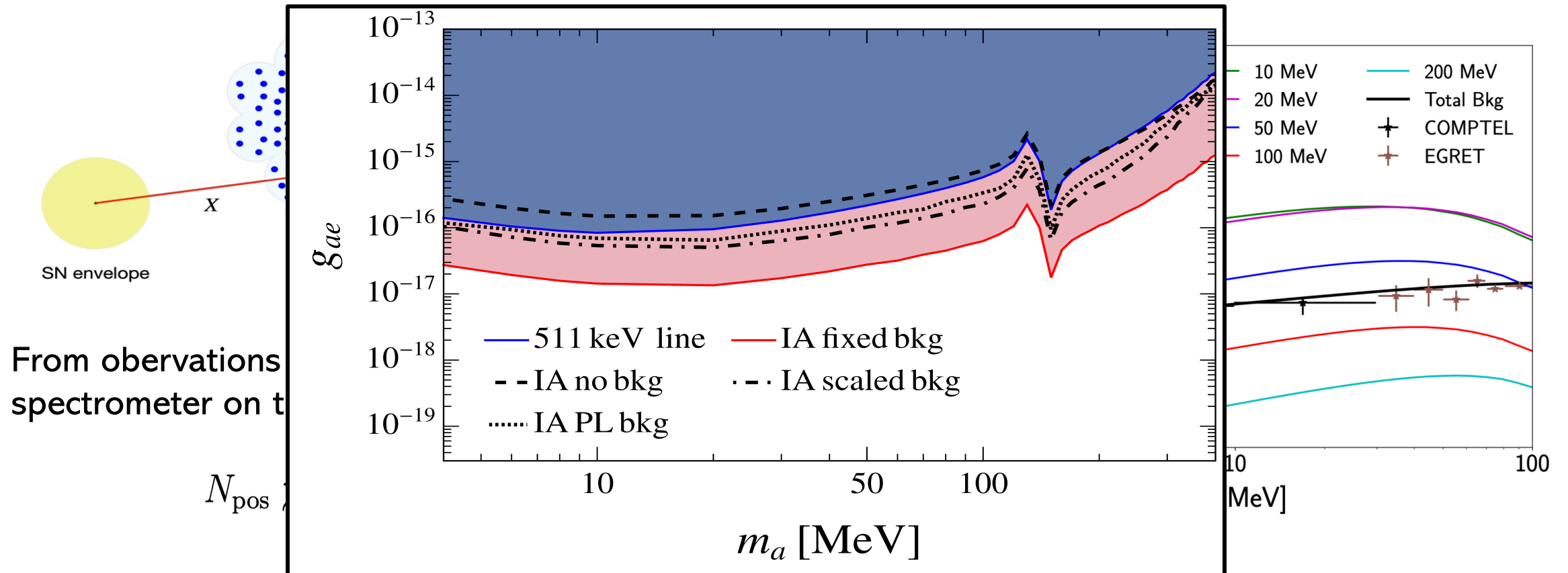
- $\lambda_e > R_{\text{env}}$
 - 511 keV line
 - In-flight annihilation

- $\lambda_e < R_{\text{env}}$
 - Energy deposition

ALP decays

ALP decaying in electrons may inject positrons in the intergalactic medium.

- Positrons annihilating at rest give contributions to the 511 keV signal
- Positrons annihilating in-flight may give rise to a diffuse bkg of soft gamma-rays

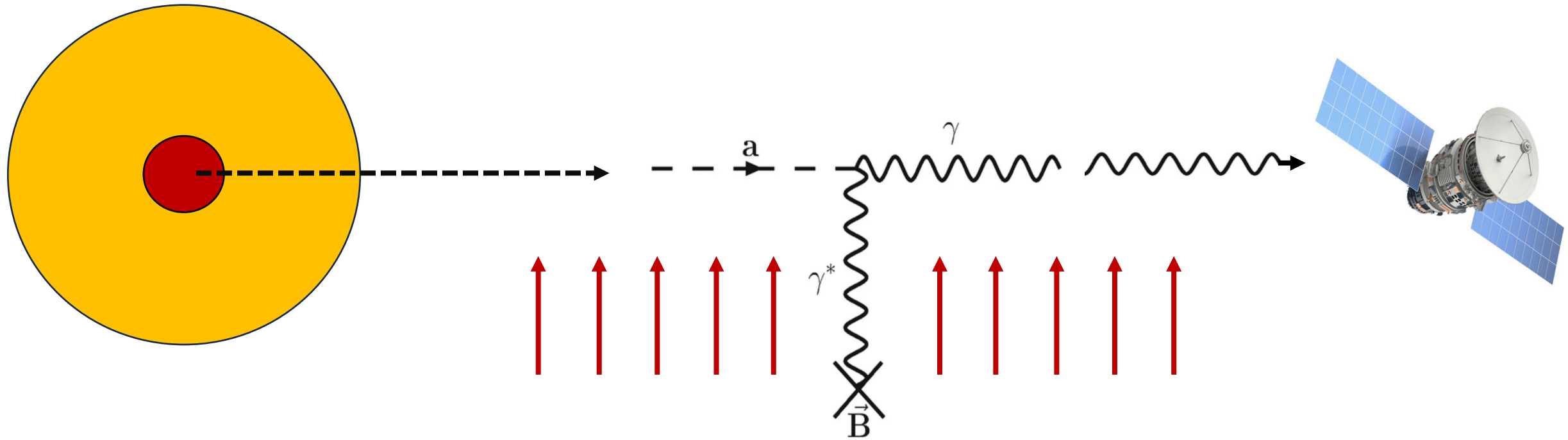


Observable signatures from conversions

$$[m_a < \mathcal{O}(1) \text{ neV}]$$

ALP conversions in B fields

Ultra-light ALPs can convert into photons in Galactic Magnetic fields



ALP conversions in B fields

Ultra-light ALPs can convert into photons in Galactic Magnetic fields

$$P_{a\gamma} = (\Delta_{a\gamma} L)^2 \frac{\sin^2(\Delta_{\text{osc}} L/2)}{(\Delta_{\text{osc}} L/2)^2}$$

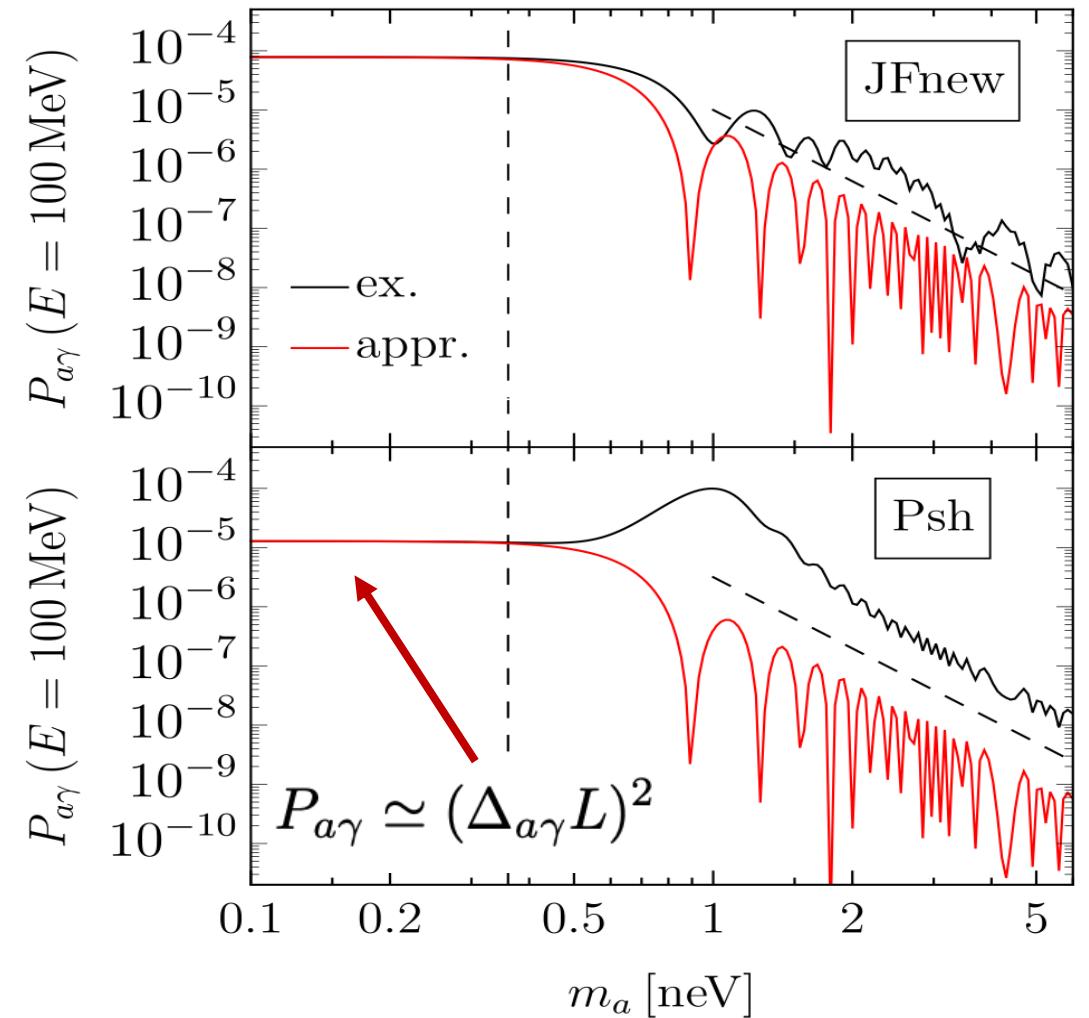
$$\Delta_{\text{osc}} \equiv [(\Delta_a - \Delta_{\text{pl}})^2 + 4\Delta_{a\gamma}^2]^{1/2}$$

$$\Delta_{a\gamma} \simeq 1.5 \times 10^{-3} \left(\frac{g_{a\gamma}}{10^{-12} \text{ GeV}^{-1}} \right) \left(\frac{B_T}{10^{-6} \text{ G}} \right) \text{ kpc}^{-1},$$

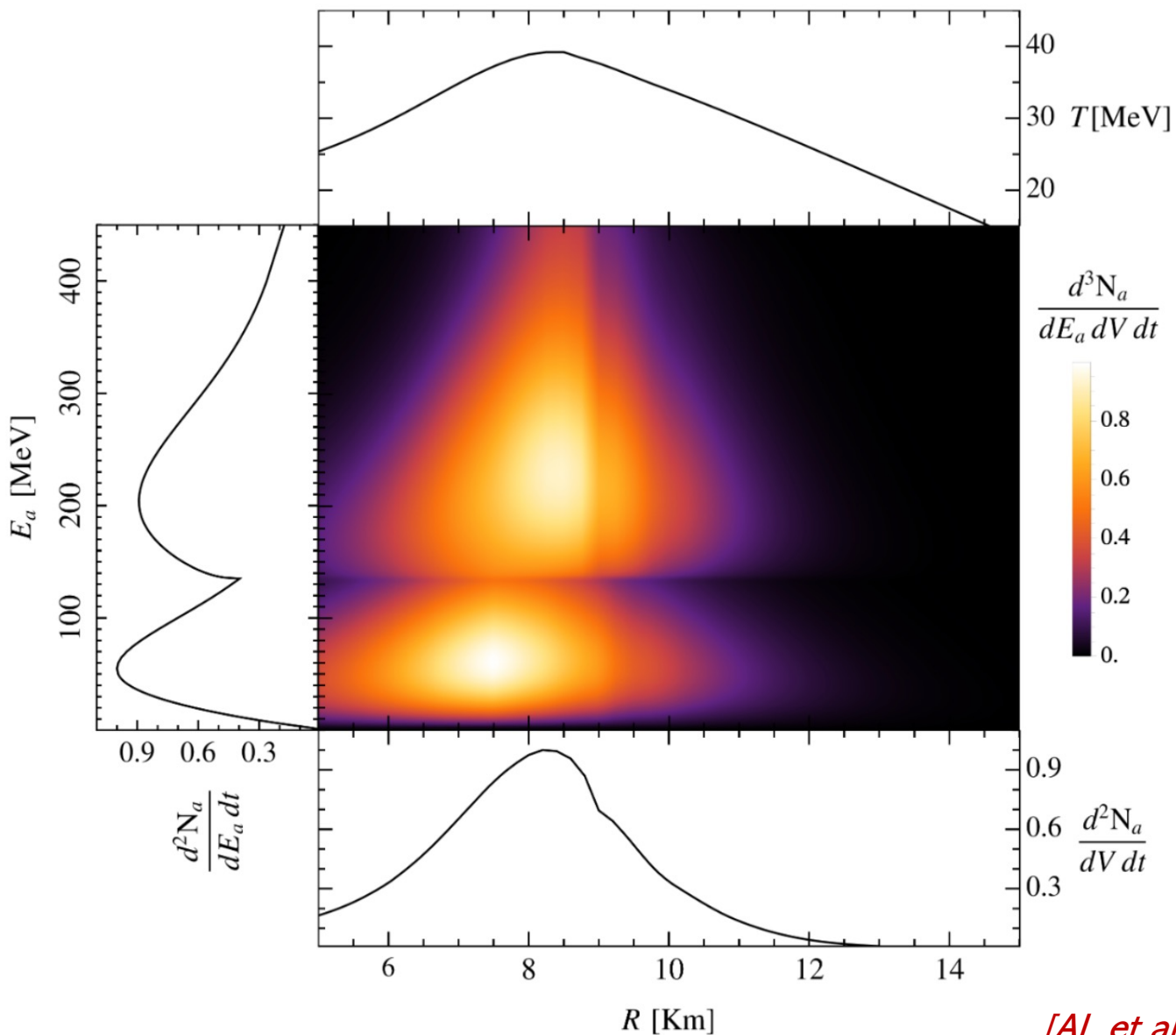
$$\Delta_a \simeq -7.8 \times 10^{-5} \left(\frac{m_a}{10^{-11} \text{ eV}} \right)^2 \left(\frac{E}{100 \text{ MeV}} \right)^{-1} \text{ kpc}^{-1}.$$

$$\Delta_{\text{pl}} \simeq -7.8 \times 10^{-7} \left(\frac{\omega_{\text{pl}}}{10^{-12} \text{ eV}} \right)^2 \left(\frac{E}{100 \text{ MeV}} \right)^{-1} \text{ kpc}^{-1}.$$

[Calore et al., Phys. Rev. D 109 (2024)]



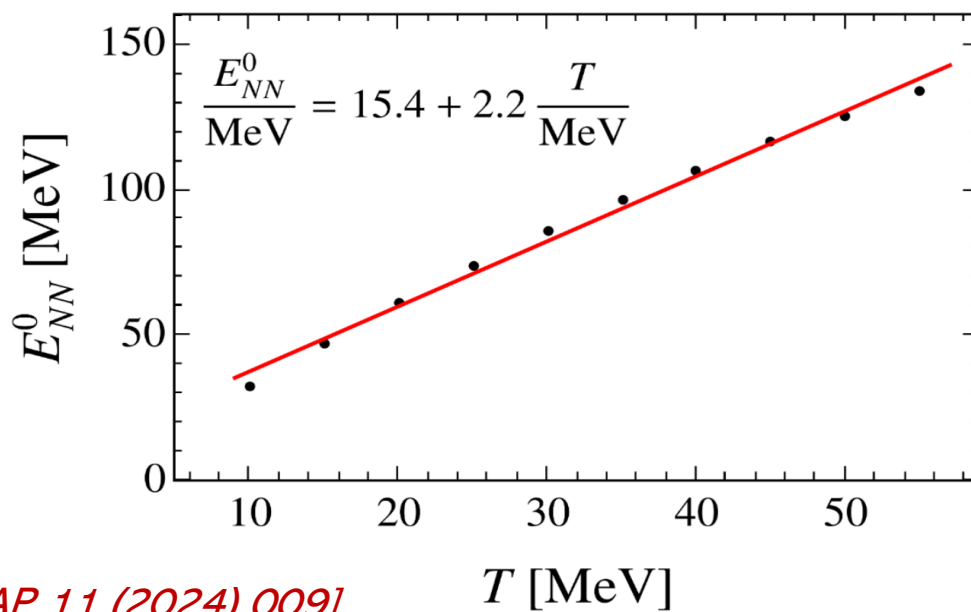
ALPs as messengers of PNS



ALPs can provide a lot of information about the PNS

$$\left(\frac{d^2 N_a}{dE_a dt} \right)_{NN} \propto \left(\frac{E_a}{E_{NN}^0} \right)^{\beta_{NN}} \exp \left[-(\beta_{NN} + 1) \frac{E_a}{E_{NN}^0} \right]$$

$$\left(\frac{d^2 N_a}{dE_a dt} \right)_{\pi N} \propto \left(\frac{E_a - \omega_c}{E_{\pi N}^0} \right)^{\beta_{\pi N}} \exp \left[-(\beta_{\pi N} + 1) \frac{E_a - \omega_c}{E_{\pi N}^0} \right]$$

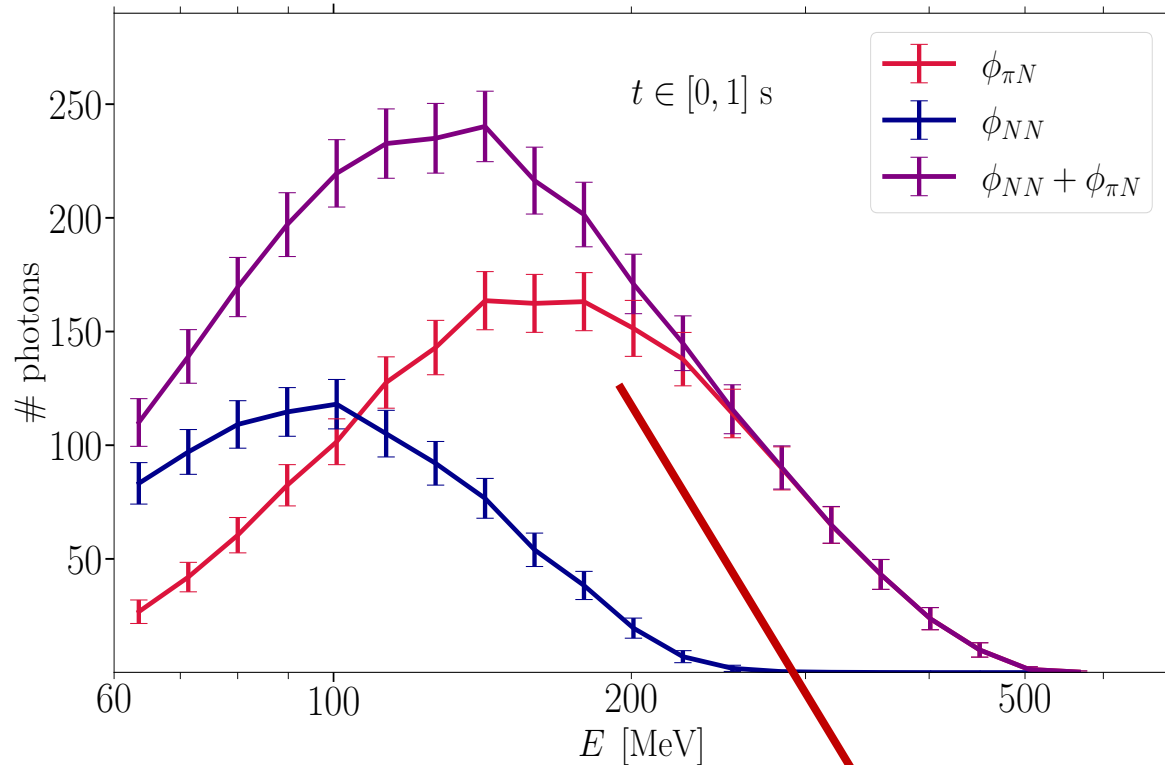


[AL et al., JCAP 11 (2024) 009]

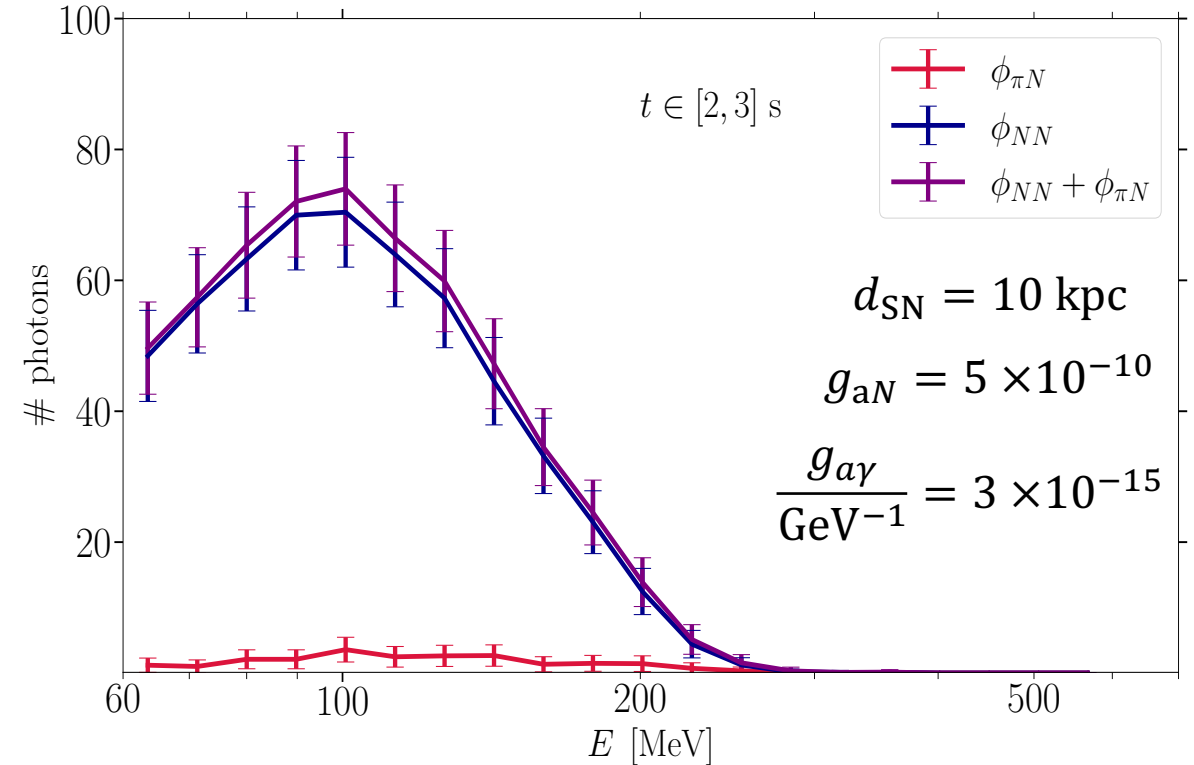
Fermi-LAT reconstruction of the signal

The ALP induced gamma-ray burst might be detected by the Fermi-LAT experiment

[AL et al., JCAP 11 (2024) 009]



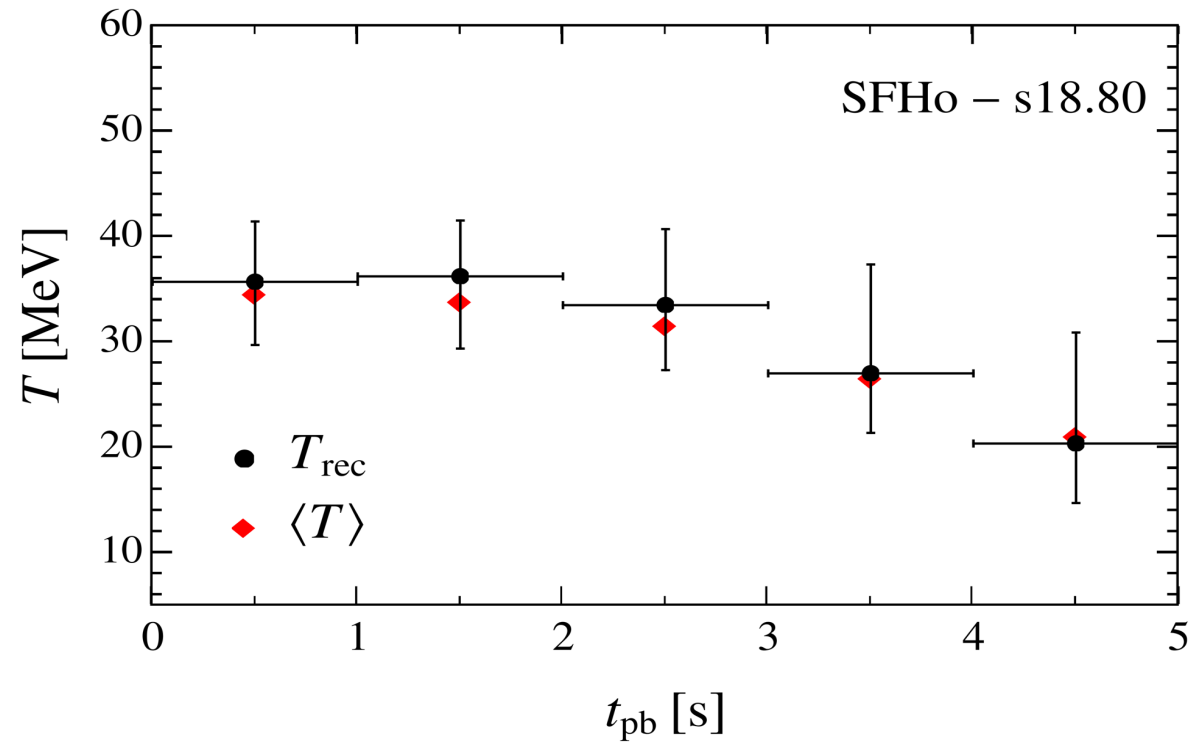
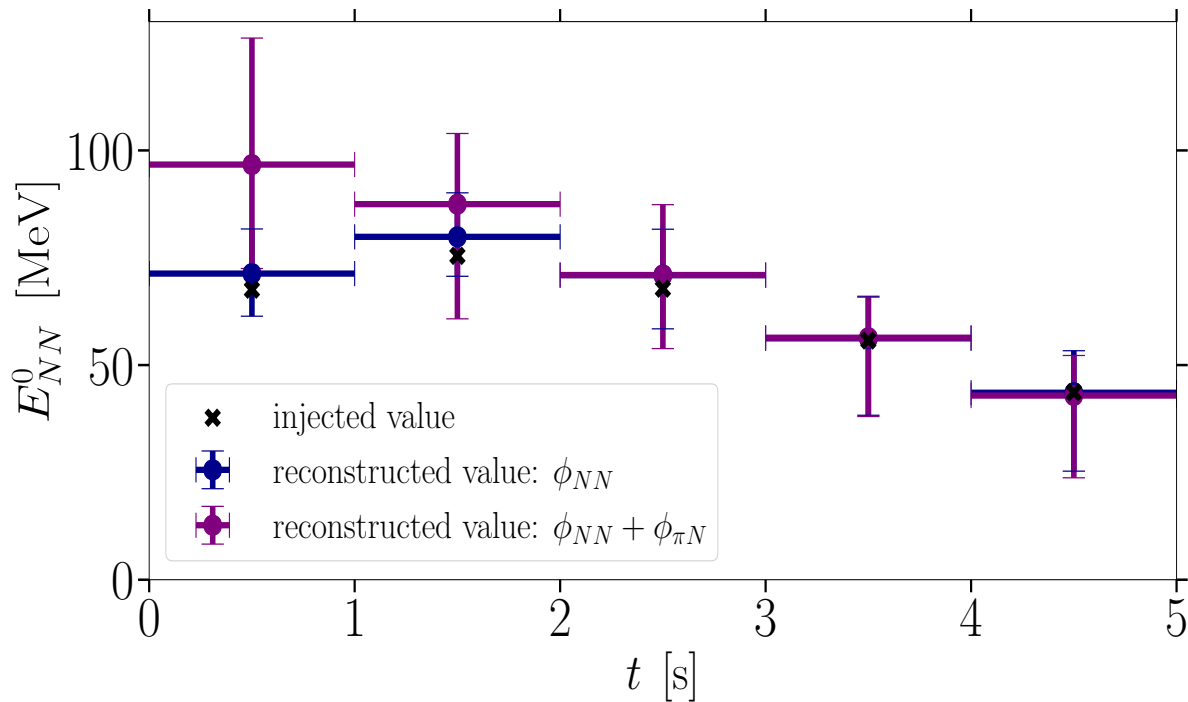
Evidence for the presence of pions in the core



Suppression of πN peak at $t_{pb} > 2$ s.

Fermi-LAT reconstruction of the signal

From parameter reconstruction one can estimate the average PNS temperature with high precision



[AL et al., JCAP 11 (2024) 009]

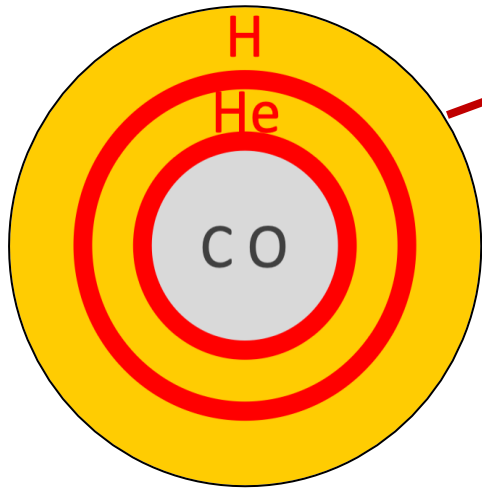
Take-home messages

- Because of the extreme conditions in the interior of the core, SNe are a powerful source of FIPs
- Axions and ALPs might be copiously produced in nuclear processes inside the SN core
- Observations of SN 1987A neutrino burst severely constrain ALP production mechanism
- A vast phenomenology for ALPs coupled with photons and electrons.
- What could we learn about SN conditions?

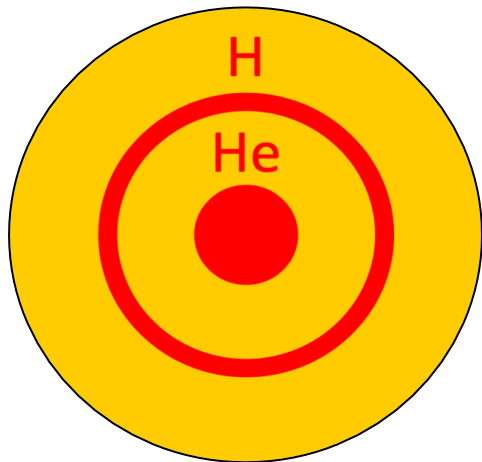
A night sky with the Milky Way galaxy visible, a silhouette of a tree in the foreground, and a dark landscape below.

**Thank you for your
attention**

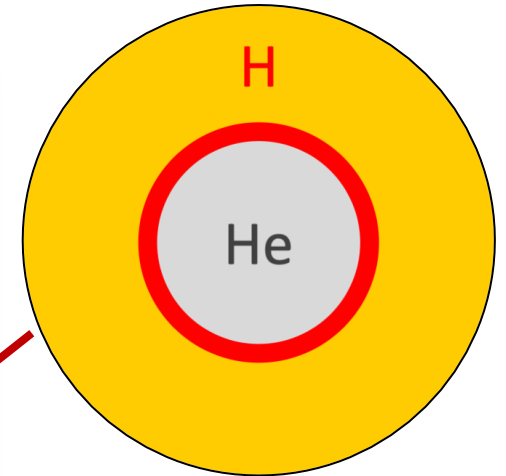
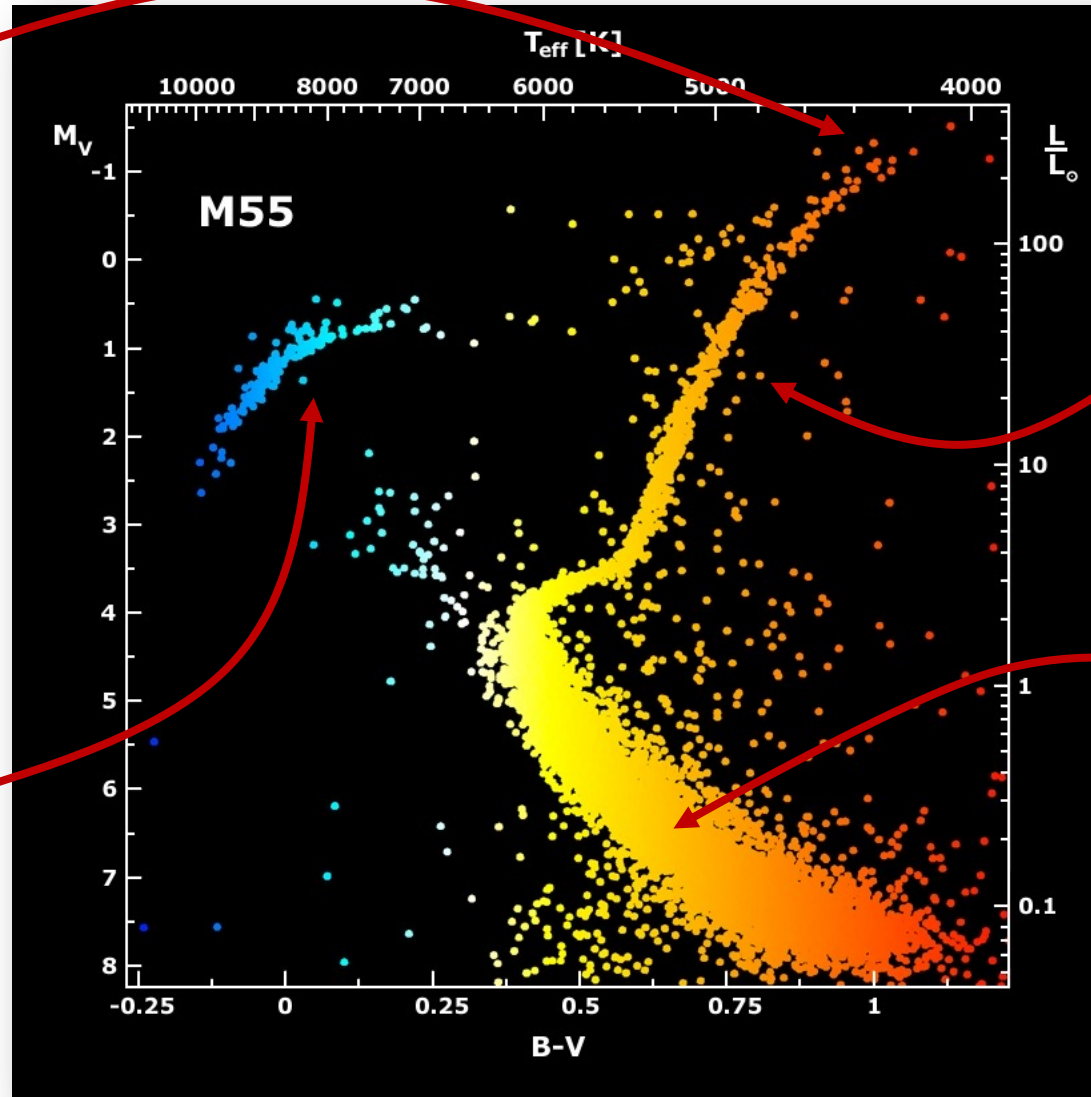
Low-mass stars ($M \leq 8M_{\odot}$)



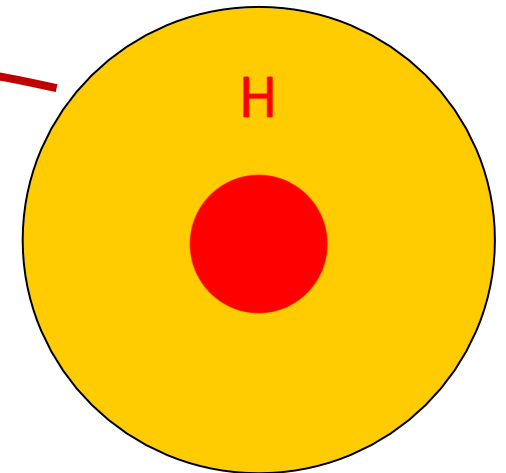
Asymptotic Giants



Horizontal Branch



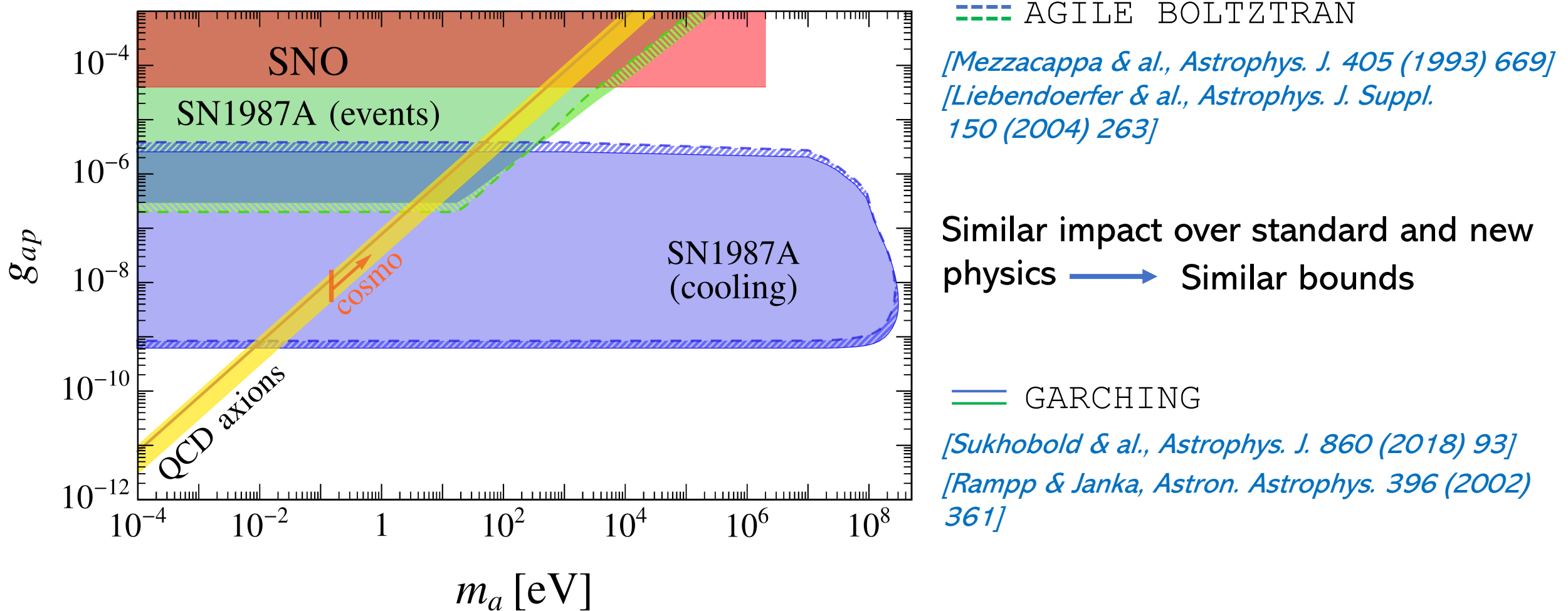
Red Giants



Main Sequence

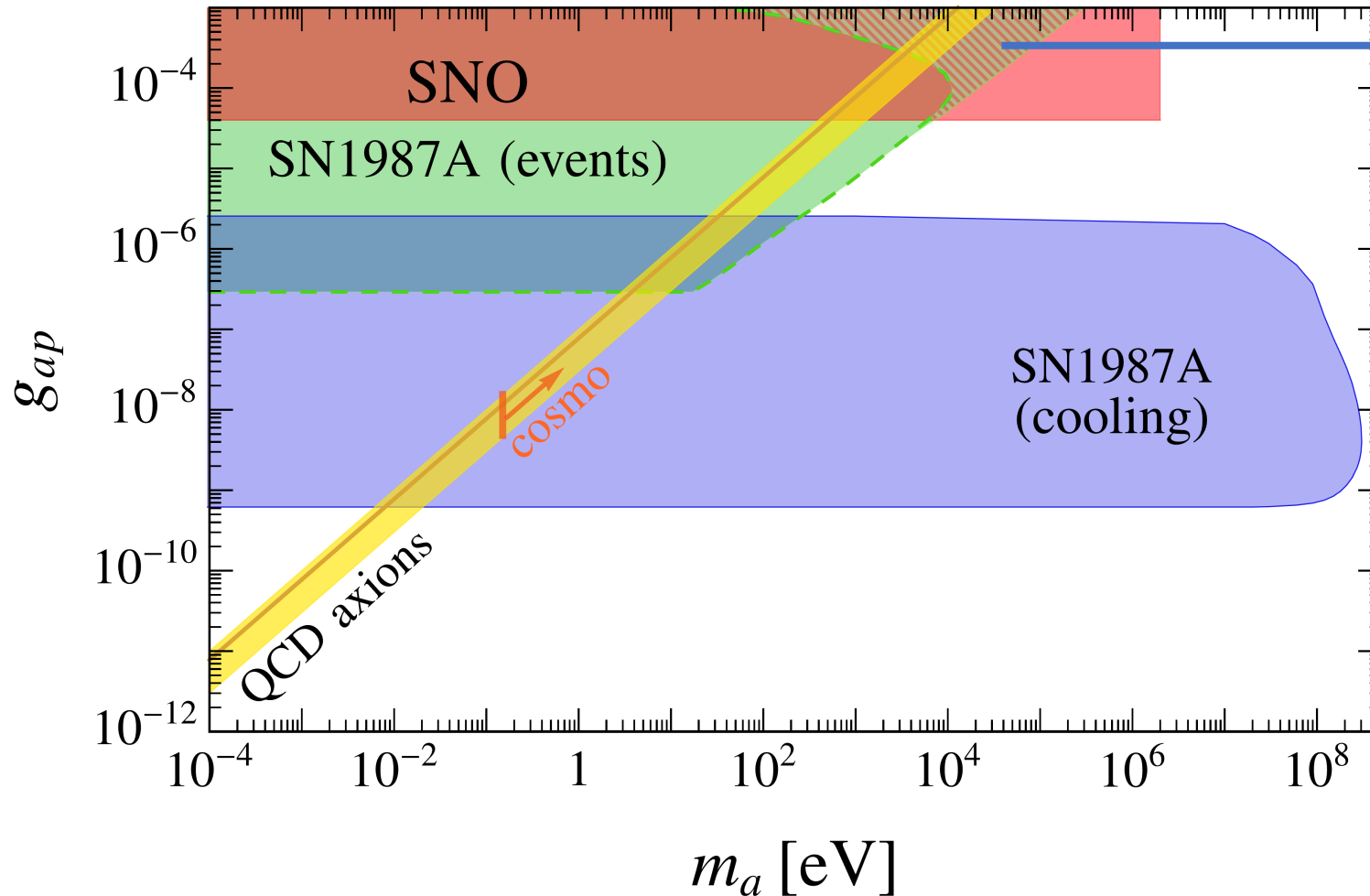
Uncertainties on SN bounds

Different SN models from same progenitors ($18.88 M_{\odot}$) show different temperature and density profiles.



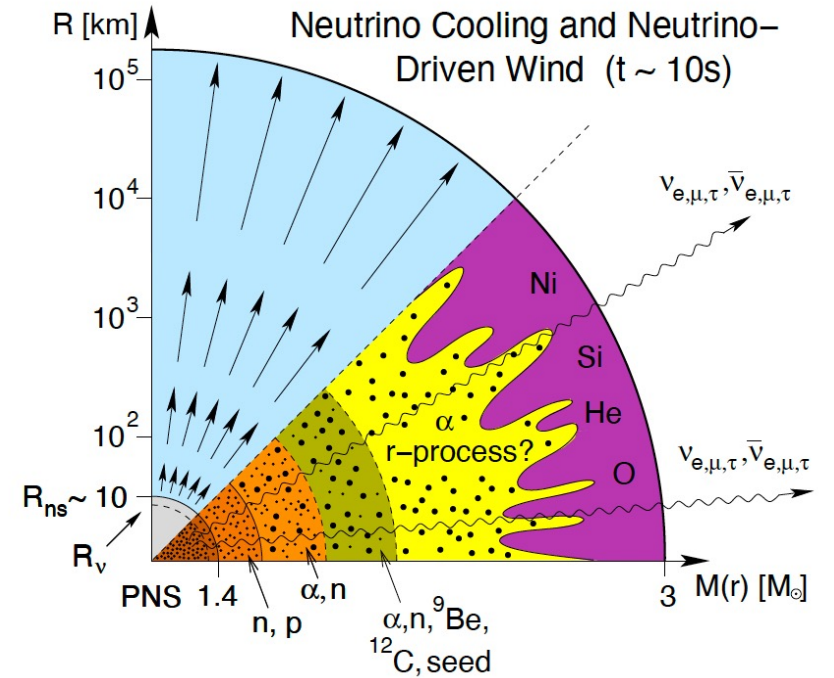
Uncertainties on SN bounds

At very high couplings, escaping ALPs can be absorbed by heavy nuclei in the neutrino driven wind



$$\eta_H(E) = \exp \left[- \int_{R_H}^{\infty} \Gamma_H(E, r) dr \right]$$

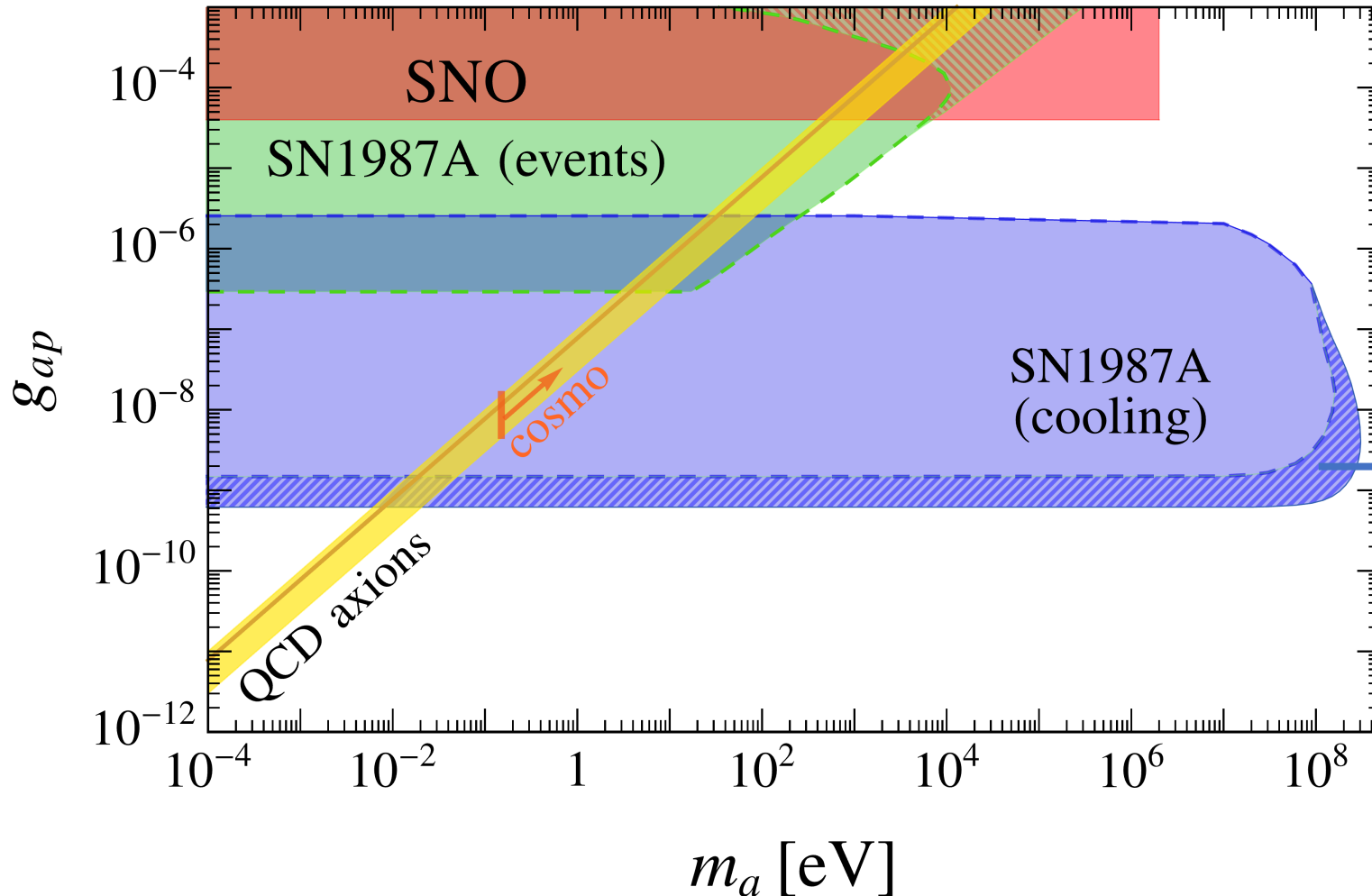
$$\Gamma_H(E, r) \sim n_H(r) \sigma(E)$$



Uncertainties on SN bounds

Strong interactions can enhance the pion fraction in the SN core

[Fore & Reddy, *Phys.Rev.C* 101 (2020) 3]



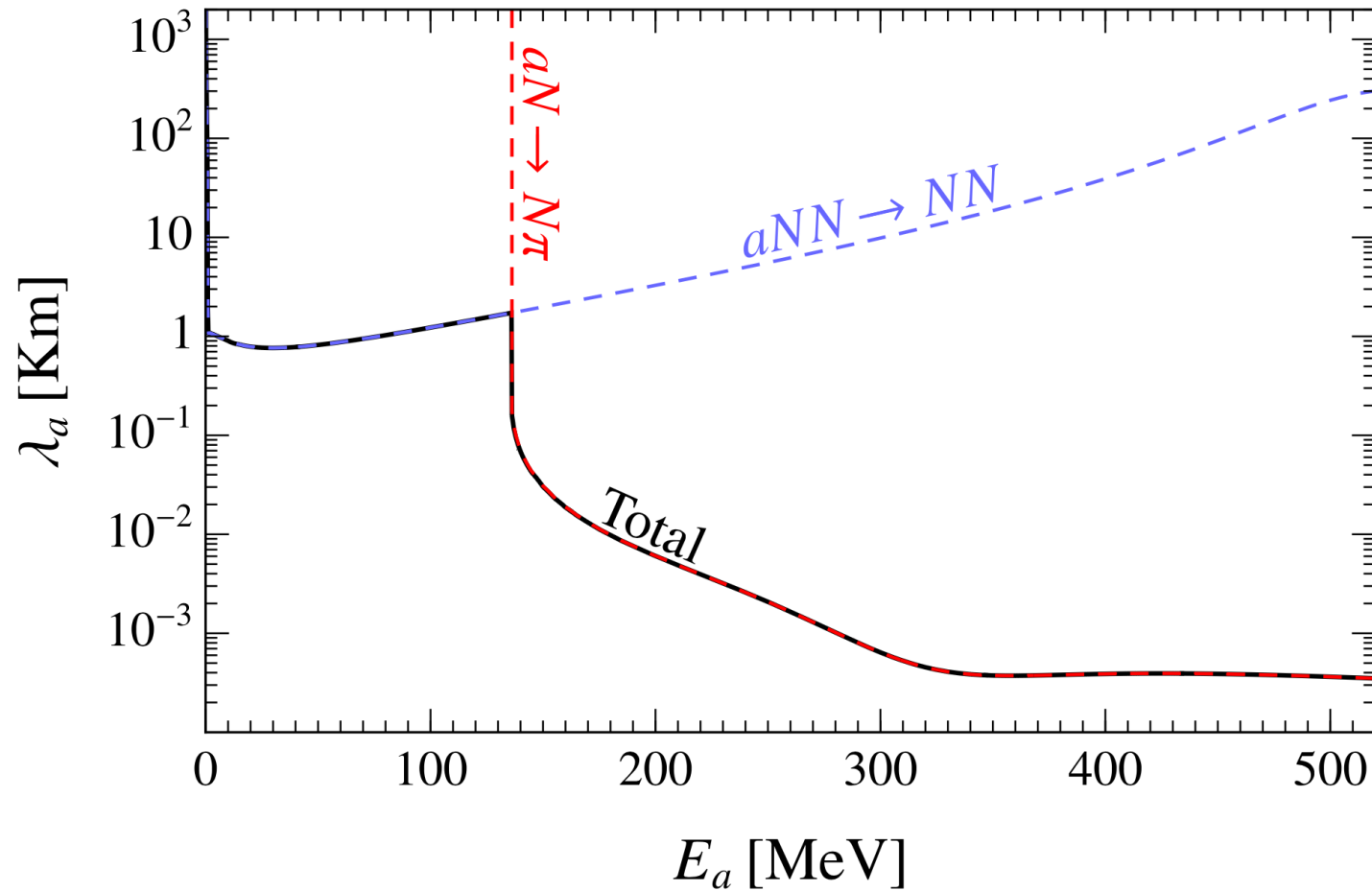
Pions still not self-consistently included in SN simulations

Fore & Reddy, e-Print: [2301.07226](https://arxiv.org/abs/2301.07226) [nucl-th]

Without pions, cooling bound relaxes by a factor ~ 2

ALP mean free path

$$\lambda_a^{-1}(E_a) = \frac{1}{2|\mathbf{p}_a|} \frac{d^2 n_a(\chi E_a)}{d\Pi_a dt}$$



Detector resolution

- Detector energy resolution spreads detected energies around true photon energies.

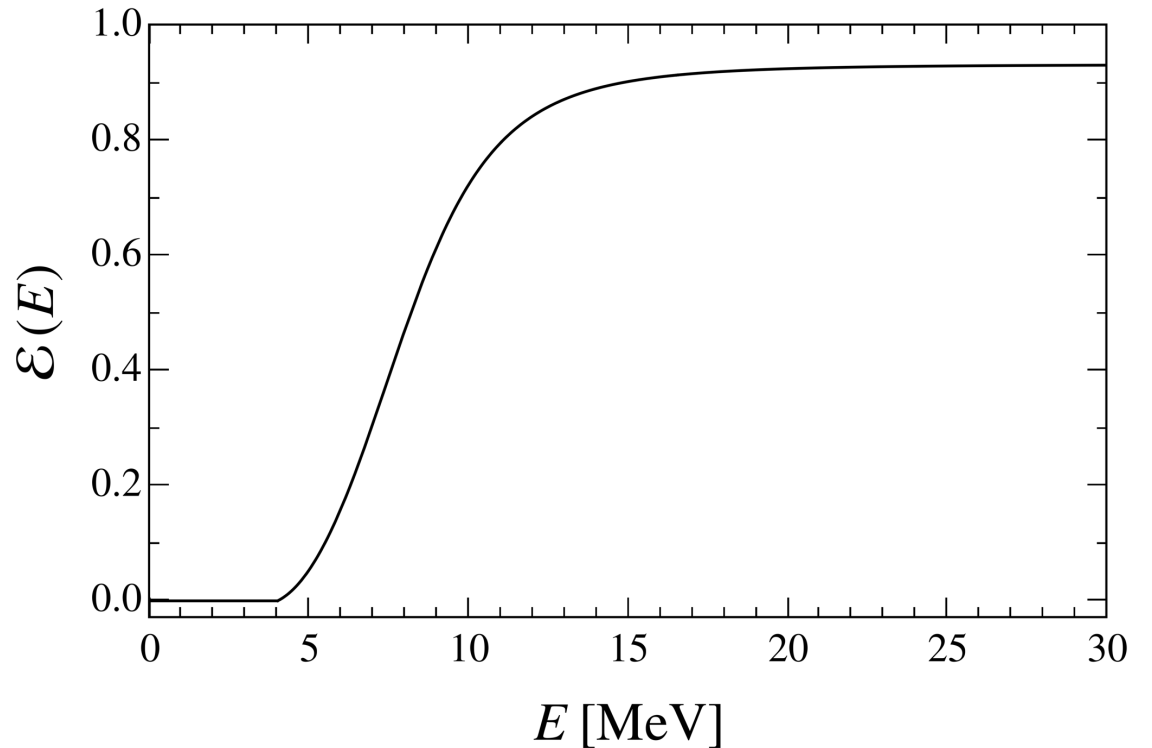
$$\mathcal{R}(E, \epsilon) = \sum_{\omega(\epsilon)} \frac{1}{\sqrt{2\pi\sigma^2}} e^{-(E-\omega(\epsilon))^2/2\sigma^2} BR[\omega(\epsilon)]$$

where $\sigma_\gamma = \sqrt{0.6 E_\gamma(\epsilon) / \text{MeV}}$

- Detector efficiency can be modelled as
[Fiorillo et al., Phys. Rev. D 108 (2023)]

$$\mathcal{E} = \begin{cases} 0 & x < 4 \\ \frac{0.932}{\sqrt{1 + \left(\frac{34}{12 - 7x + x^2}\right)^2}} & x \geq 4 \end{cases}$$

where $x = E / \text{MeV}$



ALP events from SN 1987A

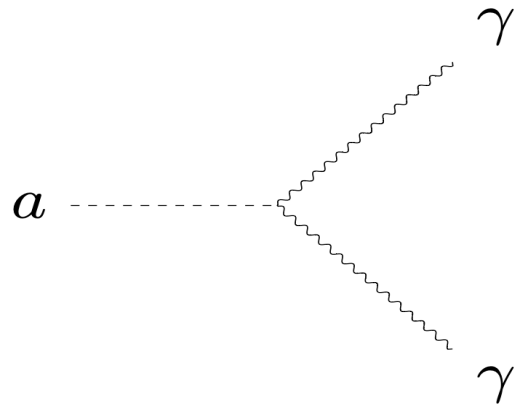
$$N_{\text{ev}} \lesssim \begin{cases} 2 \sqrt{\bar{n}_{\text{bkg}} \Delta t} & \text{if } m_a \lesssim 17 \text{ eV} \\ 2 \sqrt{\bar{n}_{\text{bkg}} \Delta t_a} & \text{if } m_a > 17 \text{ eV} \end{cases}$$

$$\Delta t \approx 12 \text{ s}$$

$$\begin{aligned} \Delta t_a(m_a) &\approx t(E_{\text{min}}, m_a) - t(E_{\text{max}}, m_a) \\ &\approx 1.82 \text{ s} \left(\frac{m_a}{10 \text{ eV}} \right)^2 \end{aligned}$$

ALP decays

- $\lambda_\gamma > R_{env}$
- γ -ray flux
- DSNALPB
- ALP basins

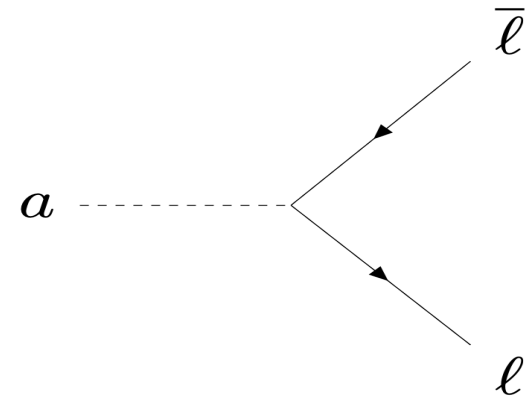


$$\lambda_\gamma = \frac{64\pi}{g_{a\gamma}^2} \frac{\sqrt{E_a^2 - m_a^2}}{m_a^4}$$

SN envelope radius $R_{env} \sim 3 \times 10^{14}$ cm

- | | |
|---------------------------------------------------------------------------------------------------------------------------|-------------------------------------------------------------------------------------------------------------------------------------------------------------------------------|
| <ul style="list-style-type: none"> ➤ $\lambda_\gamma < R_{env}$ • Energy deposition | <ul style="list-style-type: none"> ➤ $\lambda_\gamma > R_{env}$ • γ-ray flux • DSNALPB • ALP basins |
|---------------------------------------------------------------------------------------------------------------------------|-------------------------------------------------------------------------------------------------------------------------------------------------------------------------------|

$$\mathcal{L}_{al} = \sum_{l=e,\mu} \frac{g_{al}}{2m_l} (\bar{l} \gamma_\mu \gamma_5 l) \partial^\mu a$$



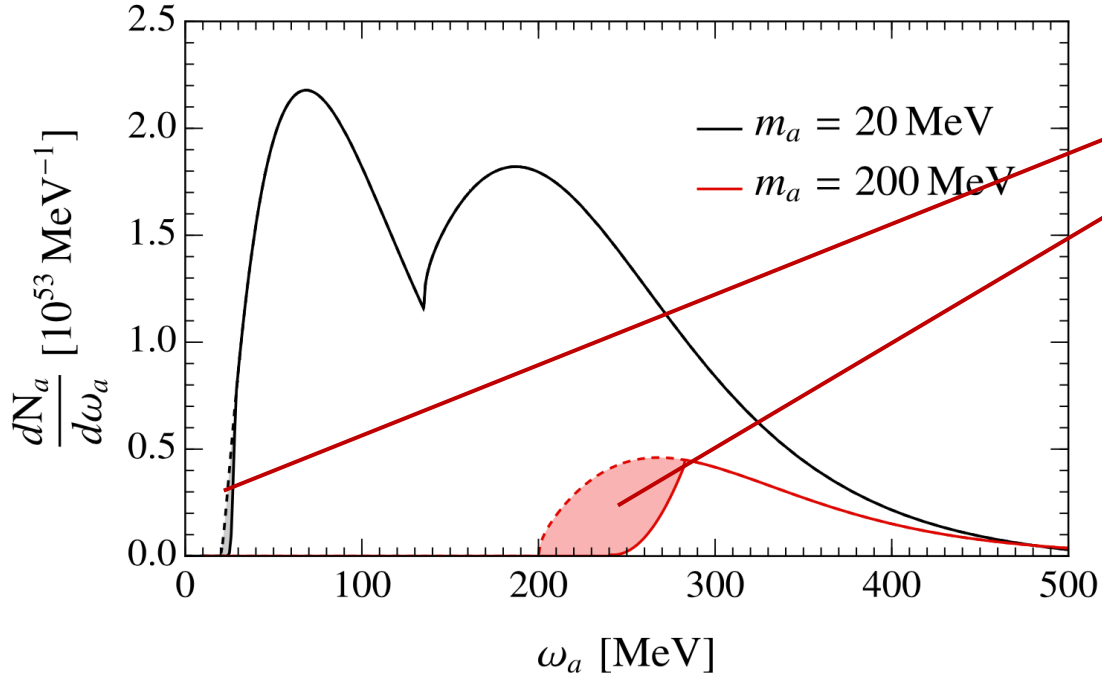
$$\lambda_l = \frac{8\pi}{g_{al}^2 m_a} \sqrt{\frac{E_a^2 - m_a^2}{m_a^2 - 4m_l^2}}$$

SN envelope radius $R_{env} \sim 3 \times 10^{14}$ cm

- | | |
|---------------------------------------------------------------------------------------------------------------------------|-------------------------------------------------------------------------------------------------------------------------------------|
| <ul style="list-style-type: none"> ➤ $\lambda_\gamma < R_{env}$ • Energy deposition | <ul style="list-style-type: none"> ➤ $\lambda_\gamma > R_{env}$ • 511 keV line • CXB |
|---------------------------------------------------------------------------------------------------------------------------|-------------------------------------------------------------------------------------------------------------------------------------|

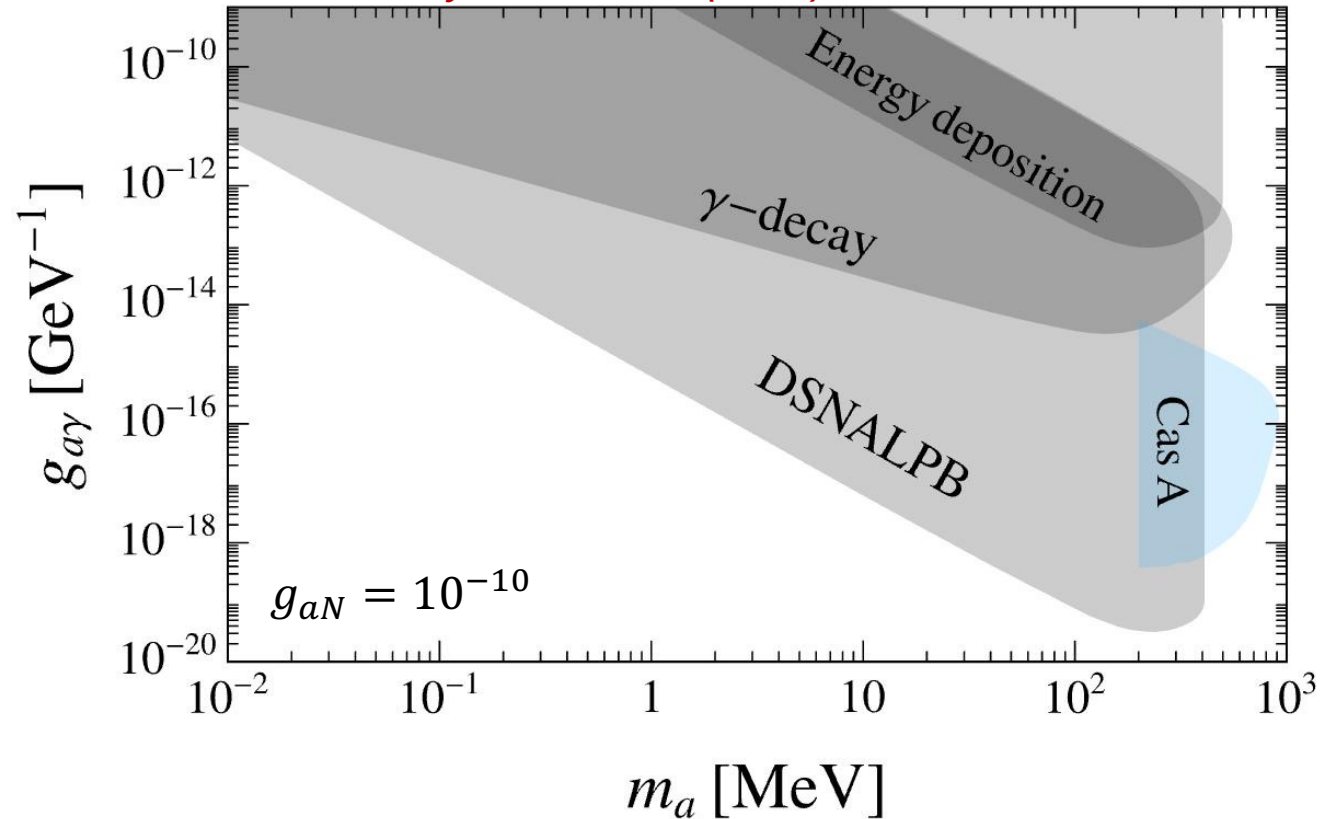
ALP Basins around SN remnants

[Hannestad & Raffelt, Phys. Rev. Lett. 88 (2002)]



Massive ALPs could remain trapped inside the PNS gravitational potential. Then, they decay at rest.

AL & al., Phys. Rev. D 107 (2023)



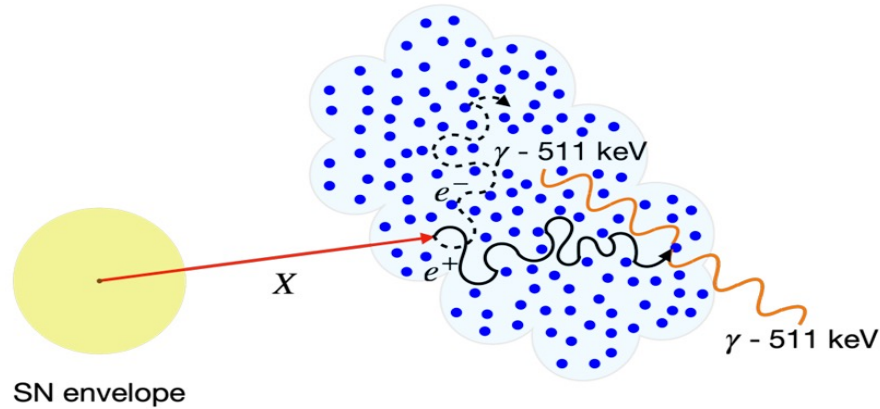
SN remnant Cas A ($d \approx 3.4 \text{ kpc}$, $t \approx 320 \text{ yrs}$).
No photon flux has been observed by Fermi-LAT:

$$\phi_{E > 100 \text{ MeV}} \lesssim 2 \times 10^{-8} \text{ cm}^{-2} \text{ s}^{-1}$$

511 keV line

[Calore et al. , Phys. Rev. D 105 (2022) 4]

[Calore et al. , Phys. Rev. D 105 (2022) 6]



ALP leptonic decays would inject positrons in the interstellar medium. By annihilating with electrons, they may give rise to a photon signal at 511 keV.

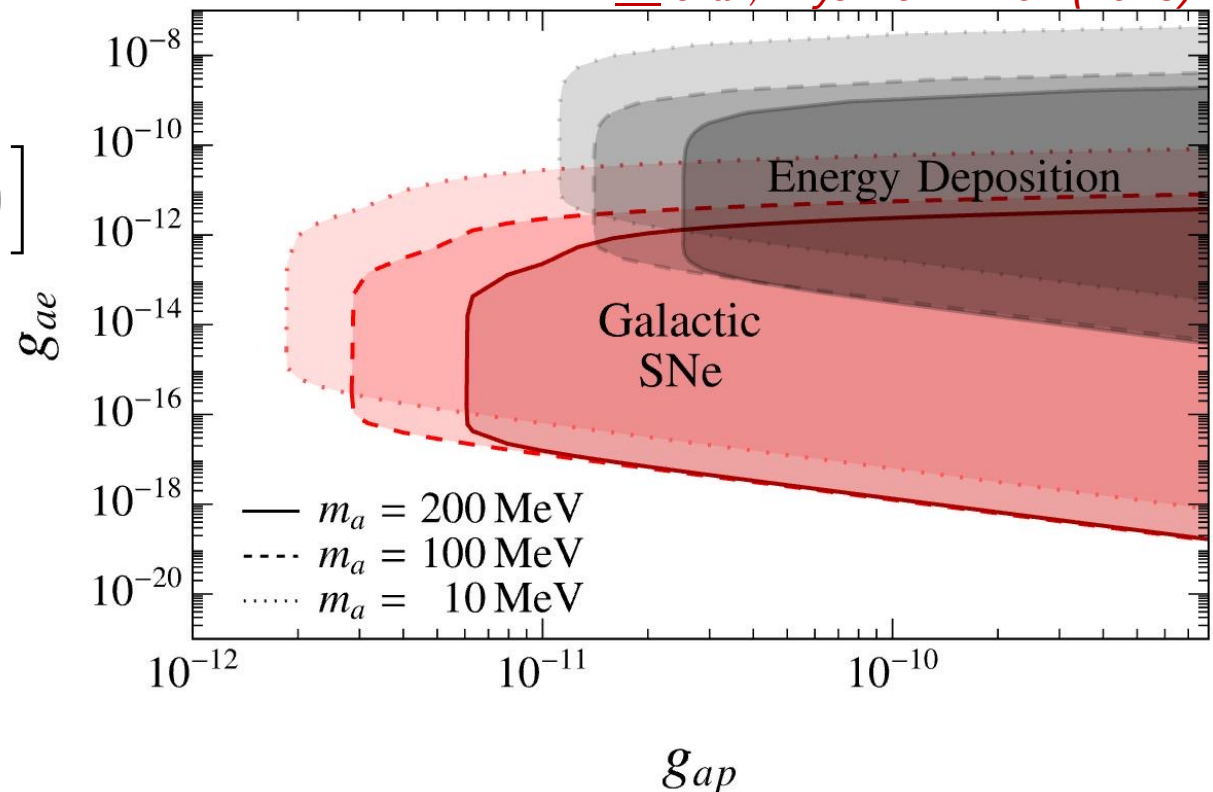
AL & al., Phys. Rev. D 107 (2023)

$$N_{\text{pos}} = \int d\omega \frac{dN_a}{d\omega} \left(\epsilon_{II} e^{-R_{\text{env}}^{II}/\lambda_e} + \epsilon_I e^{-R_{\text{env}}^I/\lambda_e} \right) \left[1 - \exp\left(-\frac{r_G}{\lambda_e}\right) \right]$$

with $R_{\text{env}}^{II} \sim 3 \times 10^{14}$ cm, $R_{\text{env}}^I \sim 10^{12}$ cm and $r_G \sim 1$ kpc.

The SPI gamma-ray spectrometer on the INTEGRAL satellite provides the following constraint

$$N_{\text{pos}} \lesssim 1.4 \times 10^{52}$$



Cosmic X-Ray Background

[Calore et al. , Phys. Rev. D 105 (2022) 6]

If ALPs are produced in extragalactic SNe, the signal from annihilation is redshifted and contributes to the CXB

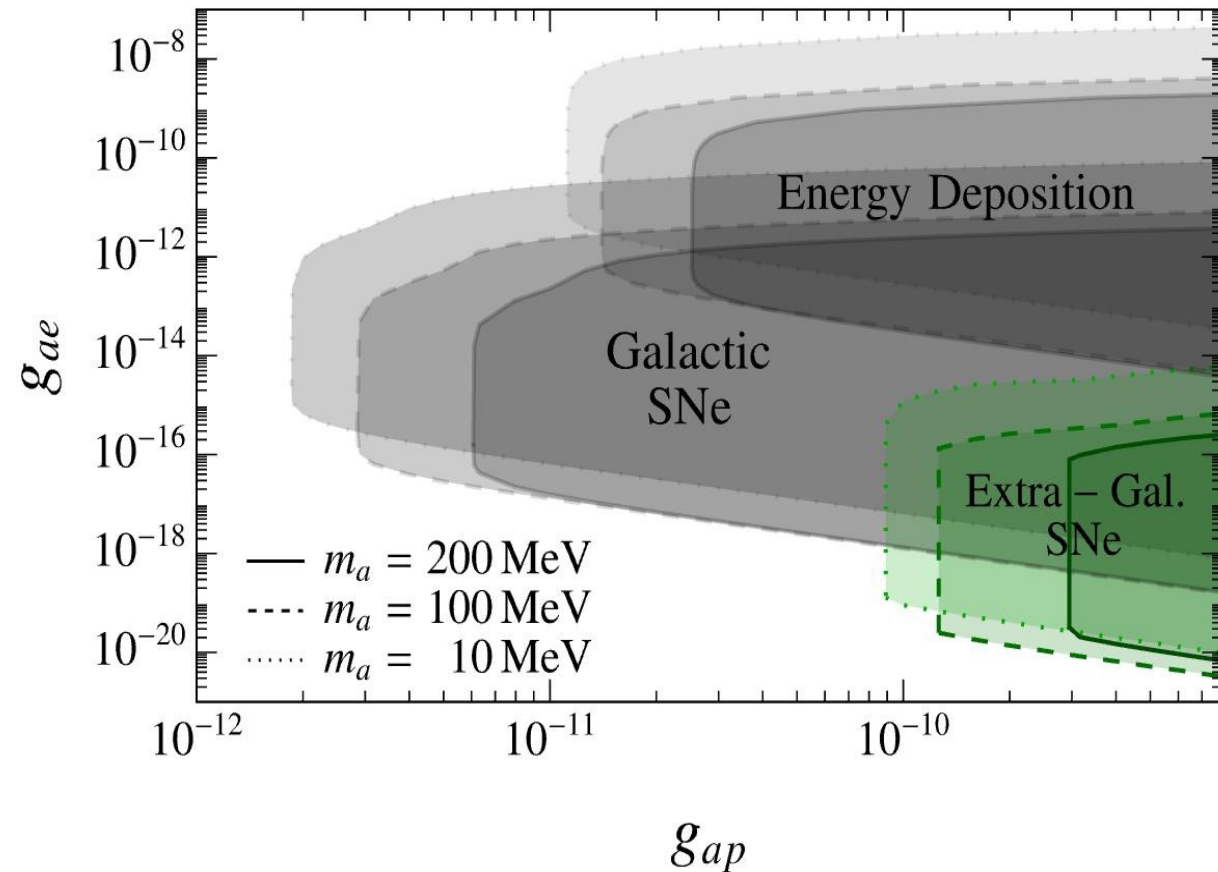
$$\frac{d\phi_\gamma}{dE_\gamma} = 2k_{ps} \frac{m_e}{E_\gamma^2} \int_{m_a}^{\infty} dE_a \frac{d^2\phi_a(E_a)}{dE_a dz_d}$$

Where

$$\frac{d^2\phi_a}{dE_a dz_d} = \int_{z_d}^{\infty} (1+z) \frac{dN_a(E_a(1+z))}{dE_a} e^{-\frac{z-z_d}{H_0\lambda_e}} \frac{R_{SN}(z)}{H_0\lambda_e} \left| \frac{dt}{dz} \right| dz$$

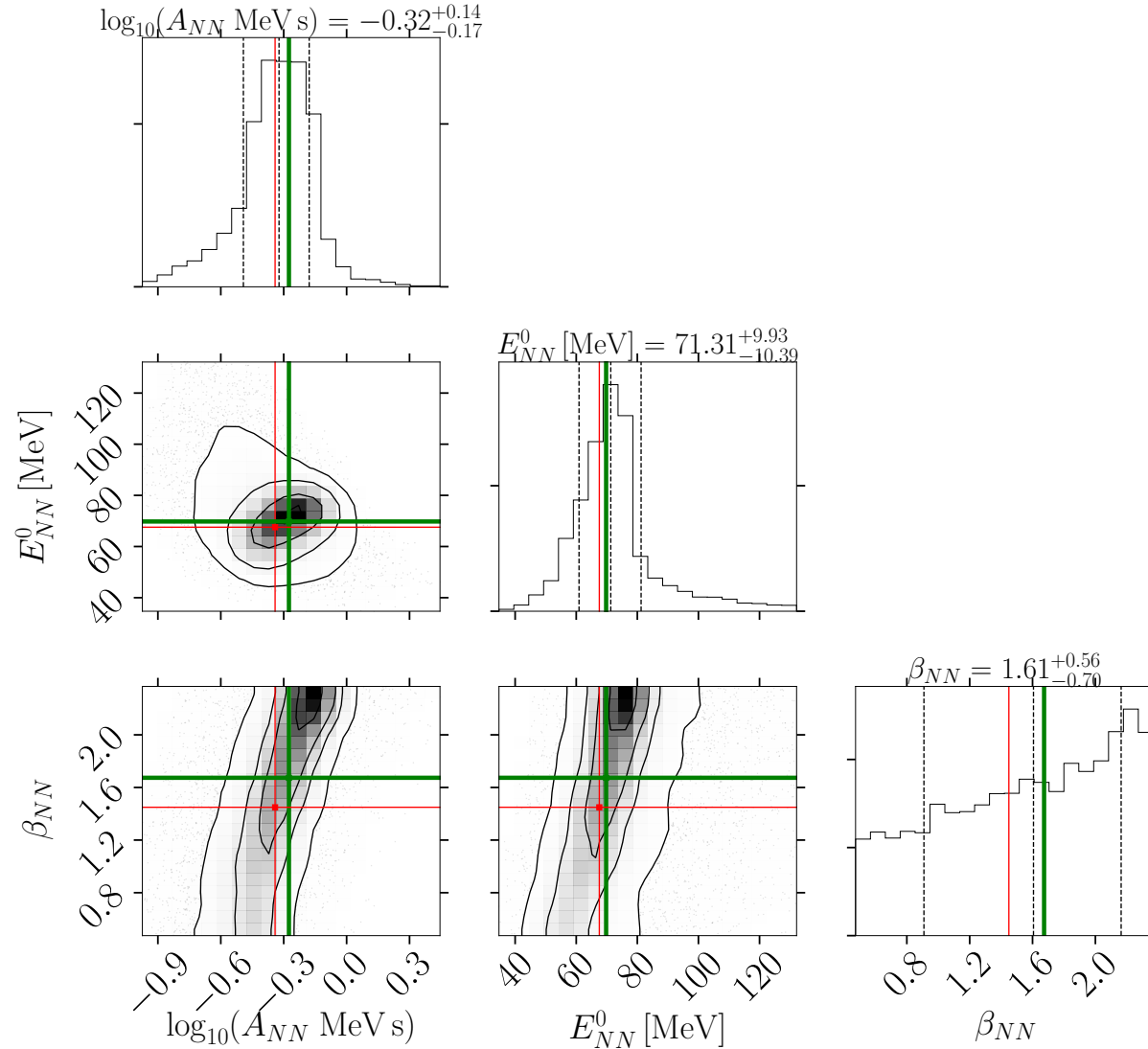
The induced CXB flux must not exceed the measurements by HEAO-1 and SMM experiments.

[AL & al., Phys. Rev. D 107 (2023)]



Fermi-LAT reconstruction of the signal

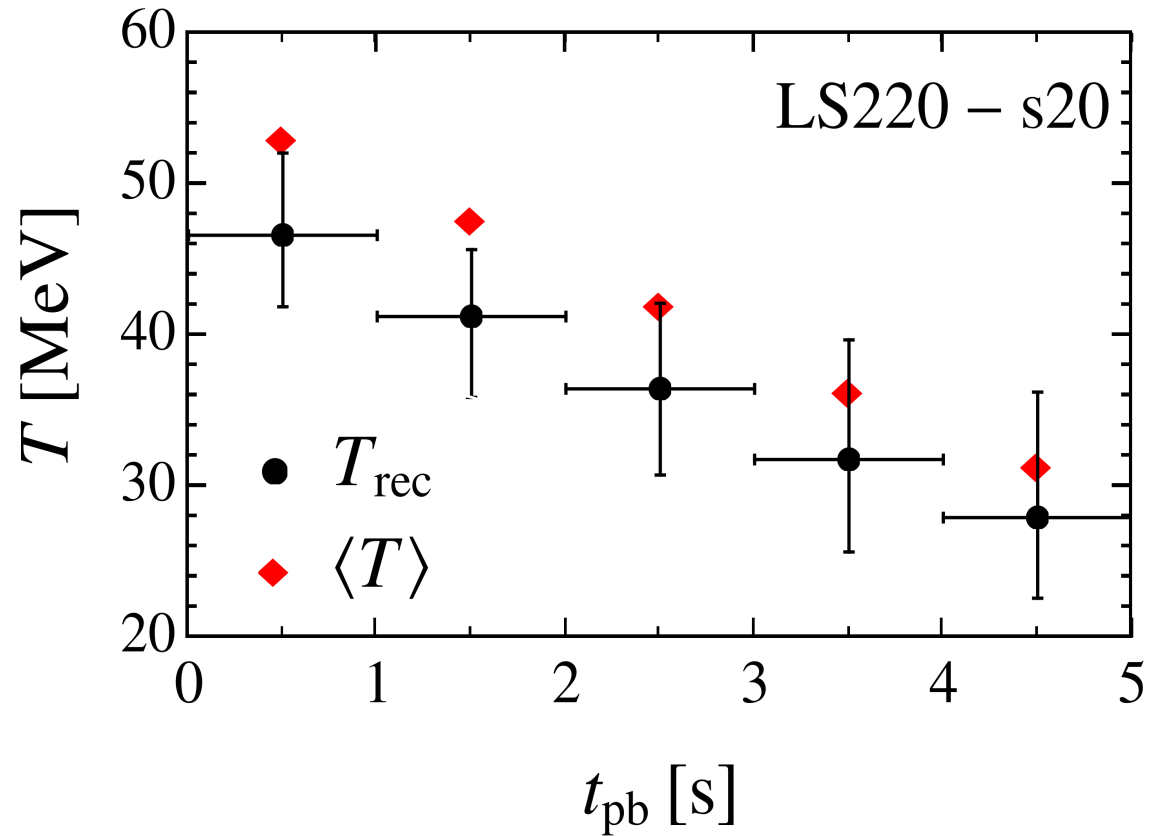
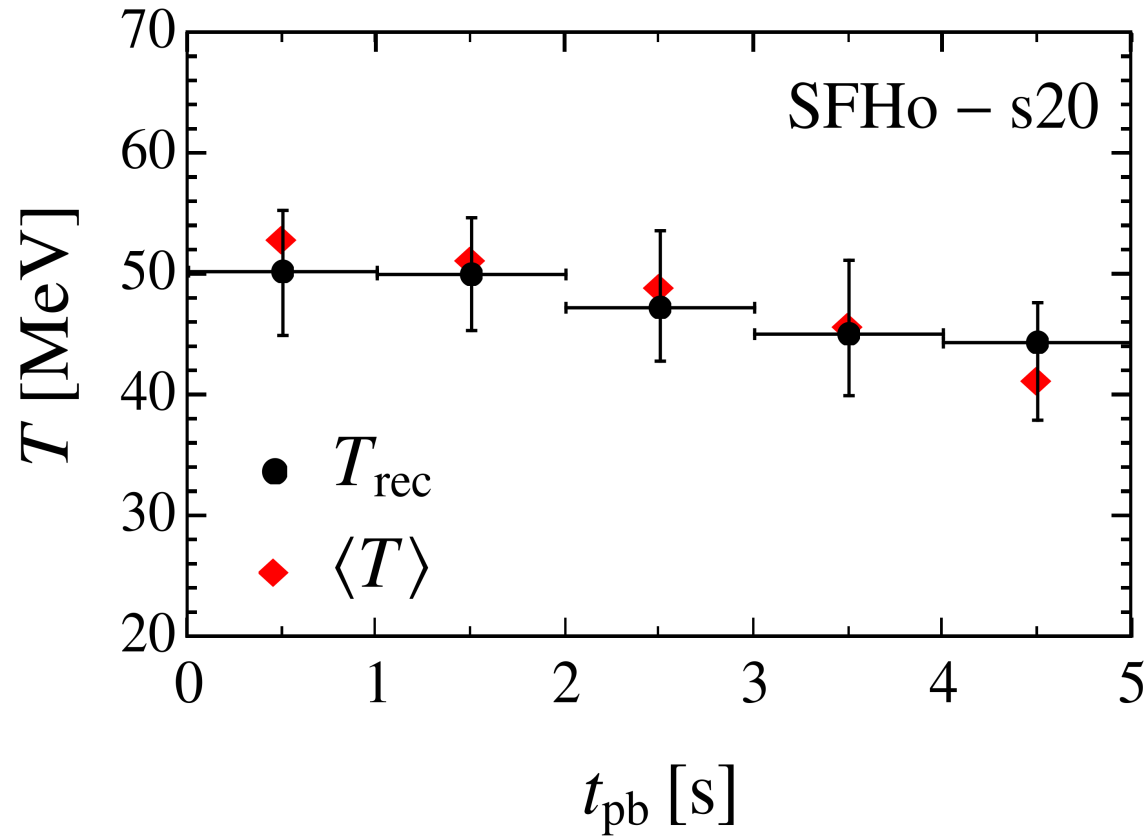
Parameter reconstruction in time interval [0, 1] s



[AL et al., JCAP 11 (2024) 009]

Fermi-LAT reconstruction of the signal

Temperature reconstruction still works for other SN models.



[AL et al., JCAP 11 (2024) 009]

The UV Theory

Above $\Lambda_{QCD} \simeq 200$ MeV interactions with quark and gluons

$$\mathcal{L}_{aQCD} = c_g \frac{g_s^2}{32\pi^2} \frac{a}{f_a} G_{\mu\nu}^a \tilde{G}^{a\mu\nu} + \sum_q c_q \frac{\partial_\mu a}{2f_a} \bar{q} \gamma^\mu \gamma_5 q + \frac{(m_{a,0})^2}{2} a^2$$

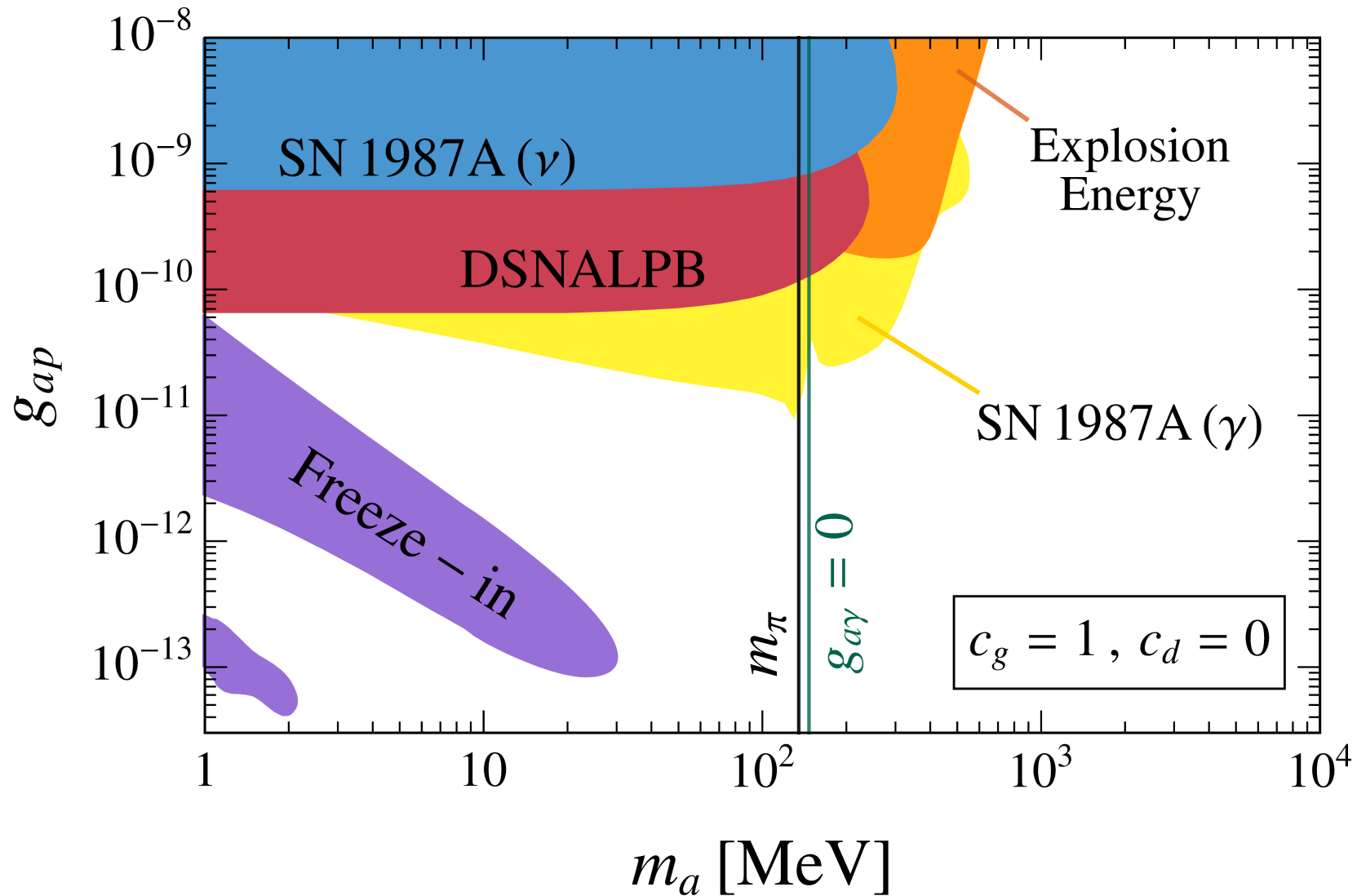
Then, at loop level [*Bauer et al., JHEP 12 (2017)*]

$$C_\gamma(c_g, c_u, c_d) = -1.92 c_g - \frac{m_a^2}{m_\pi^2 - m_a^2} \left[c_g \frac{m_d - m_u}{m_d + m_u} + (c_u - c_d) \right]$$

Irreducible photon coupling related to nuclear couplings ($C_n = 0, c_g = 1$)

$$g_{a\gamma} \simeq -9.5 \times 10^{-4} \text{ GeV}^{-1} \left[\frac{1.53}{c_d - 0.33} + \frac{c_d + 0.24}{c_d - 0.33} \frac{m_a^2}{m_\pi^2 - m_a^2} \right] g_{ap}$$

Bounds on g_{ap}



[AL & al., Phys.Rev.D 110 (2024)]